NuMI-B-542
V1.0
October 12, 1999

Proposal to Include Hadronic Hose in the NuMI Beam Line

J. Hylen, J. Walton, W. Smart, S. Childress
Fermilab
V. Garkusha, F. Novoskoltsev, V. Zarucheisky
IHEP, Protvino
M. Messier
Harvard
R. Milburn
Tufts
J. McDonald
Pittsburgh
J. Thomas
U.C. London

Abstract

The Hadronic Hose is a magnetic focusing device which would be installed in the decay pipe of the NuMI neutrino beam line. The primary motivation is to reduce the differences in the shape of the neutrino spectra at the MINOS far and near detectors. The reduction in near/far differences will reduce the systematic uncertainties in neutrino oscillation measurements.

The Hadronic Hose would consist of segments of wire, 660 m in total length, running down the center of the decay pipe. A current pulse of order 1000 Amps on the wire produces a toroidal magnetic field. The current is returned through the iron decay pipe. In this field, pions orbit with trajectories that sweep their neutrino decay fluxes across the centers of the near and far detector which helps to average out near and far differences.

Side benefits of the Hadronic Hose are to increase the neutrino flux of the low energy beam configuration and to modestly loosen alignment tolerances.

Contents

1 Near and Far Spectra

A design feature of the MINOS experiment is to have nearly identical detectors in two locations, one near the source of neutrinos, and the other far away. Features such as steel thickness and scintillator thickness are made the same, so that systematic uncertainties in event identification and neutrino cross section will cancel in the near-far comparison.

The same principle can be applied to the neutrino beam. It is desirable that the spectra (in the absence of oscillations) near and far be as identical as possible, so that uncertainties from the lack of precise knowledge of neutrino cross sections which convolute with beam uncertainty are removed. As shown in the upper half of Figure 1, the near and far spectra of the baseline PH2ME beam are similar, but significantly different.

This proposal presents an addition to the NuMI beam line that improves the near-far spectrum comparisons. The "Hadronic Hose", which produces continuos focusing of pions and Kaons over the entire length of the decay pipe, makes the spectra in the near and far detectors much more similar, as shown in the bottom half of Figure 1. The required magnetic field is provided by inserting a current-carring wire running down the full length of the decay pipe.

2 Hadronic Hose and Beam Systematics

2.1 Sources of Near/Far Spectrum Differences

There are three basic effects that cause differences in the ν_μ energy spectrum in the MINOS near and far detectors, as shown in Figure 2:

- Since the mean distance a pion travels before decaying is given by $\gamma c\tau$, high energy pions live longer. Thus the source of high energy neutrinos is on average closer to the near detector than is the source of low energy neutrinos. This effect is exactly calculable.

- Well focused pions travel farther down the decay pipe and on average decay closer to the near detector than poorly focused pions which are absorbed on the decay pipe walls. This effect on the source distance depends on focusing misalignments and hadronic production p_t.

- Neutrinos produced from pion decays off the beam axis have a larger decay angle when directed towards the center of the near detector than the far. The difference in the decay angles increases as the radius of the pion decay increases. As lower energy neutrinos are produced at larger decay angles,

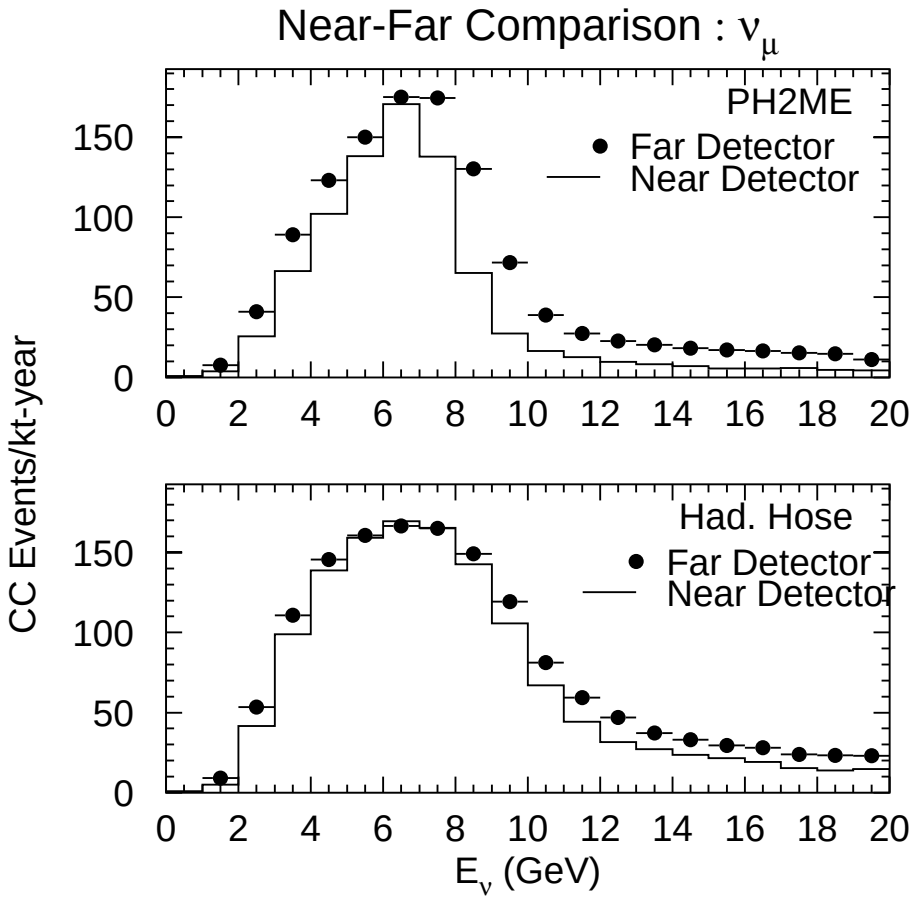

Figure 1: Top: Comparison of the ν_μ charged-current event spectrum for the baseline PH2ME beam in the Far Detector (dots) with the spectrum in the Near Detector (histogram). Bottom: same but with the addition of the Hadronic Hose. In each plot, the near detector event rate is scaled by 0.77×10^{-6}, which corresponds to the relative flux that would be expected based on the lifetime of a 10 GeV pion traveling down the center of the decay pipe.

this means that energy of neutrinos directed towards the near detector is on average lower than neutrinos directed at the far detector. This effect is sensitive to the radius in the decay pipe where the pion decays, and thus to the pion focusing and hadronic production p_t.

2.2 Hadronic Hose Concept

A way to mitigate the last two of the causes of near/far spectrum differences listed in the previous section is to provide continuous central focusing of pions in the decay pipe (after the horn focusing system). Pions are then trapped in oscillating trajectories as shown in Figure 2 and 3. A wire running down the center of the decay pipe carrying a current of order 1 kA produces sufficient magnetic field to trap most pions. The pions are kept from the decay pipe walls and the oscillating trajectories even out the decay angular distributions to the near and far detectors. The spectra produced in the near and far detectors are then much more similar, as seen in Figure 1. More importantly, systematic variations of the hadronic production p_t tend to have more similar effects in the near and far detectors, as seen in Figure 4. (This variation is described in more detail in the next section). The cancellation of the systematic uncertainties in the near/far ratio will allow the prediction of the spectrum in the far detector from the measured spectrum in the near detector to 2%.

The theory of this continuous central focusing (which we have named the "Hadronic Hose") is described in Ref. [1]. Note that the pion trajectories in the Hadronic Hose field are nearly coplaner with Hose wire, not helical, so that the direction of travel sweeps nearly through the center of the near detector. As pions orbit to small radii, the wire carrying the current must be small (of order 1 mm radius), to minimize pion absorbtion on the wire.

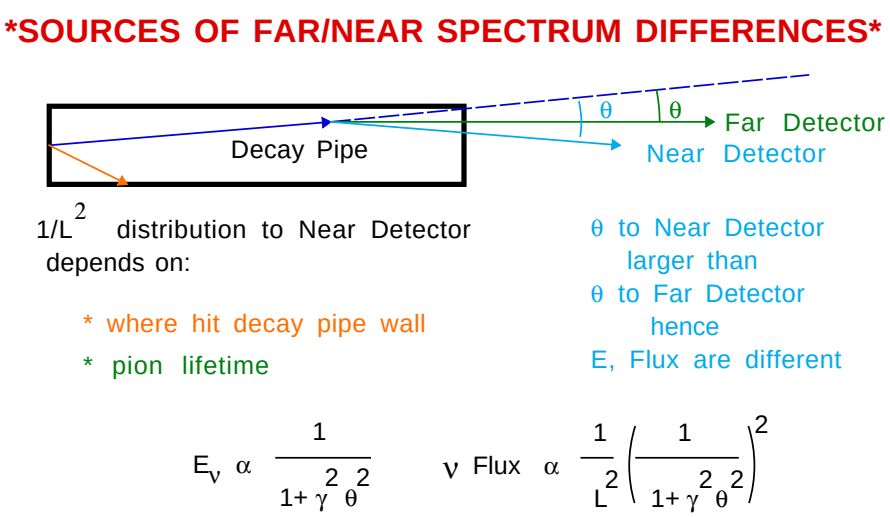

Figure 2: How Hadronic Hose reduces differences in the energy spectrum seen in the near and far detectors.

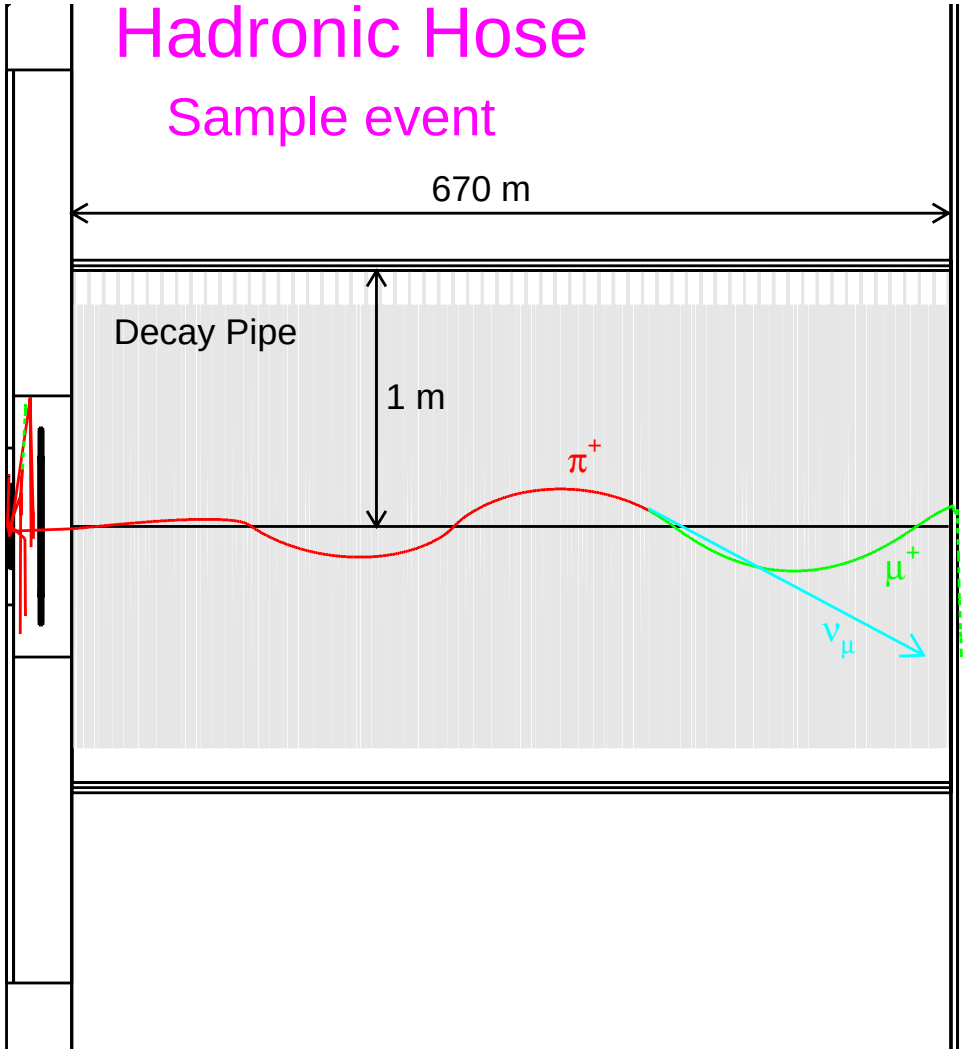

Figure 3: A `GNuMI` sample event display showing the trajectory of a π^+ which orbits the Hadronic Hose wire, and decays to $\mu^+\nu_\mu$.

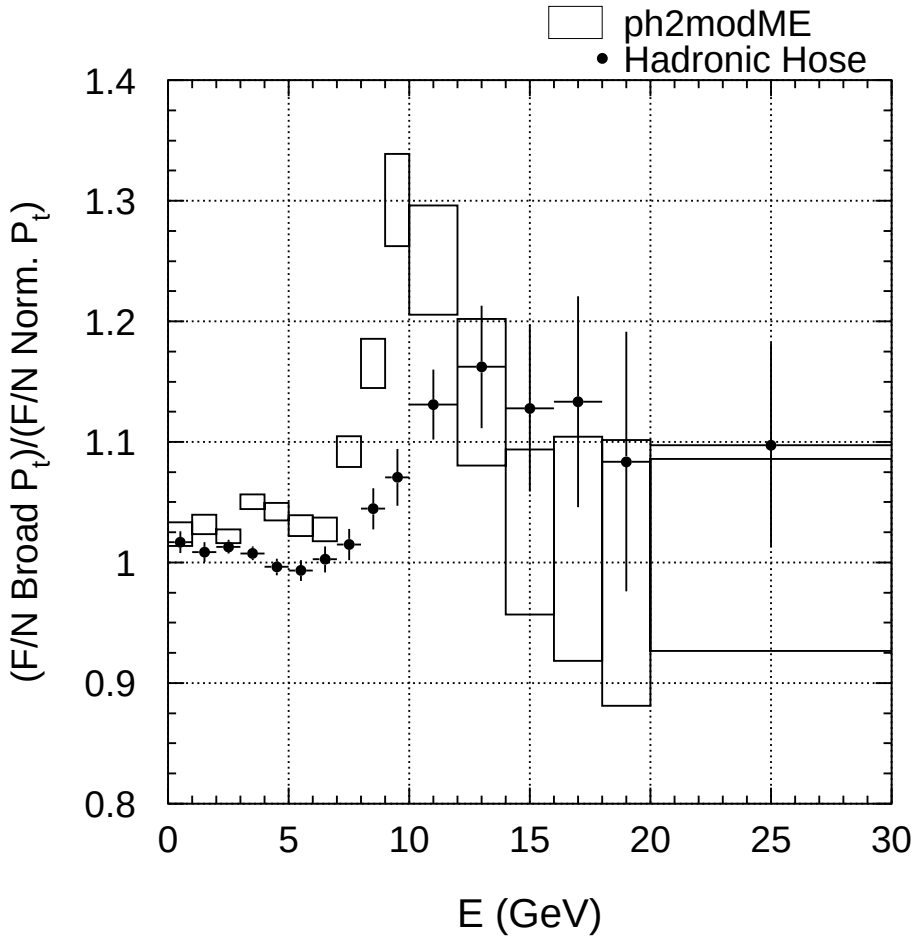

Figure 4: Relative variation in the far/near comparison when the hadronic production p_t spectrum is varied, for the basline PH2ME design (boxes) and for Hadronic Hose (points). Box size and point error bars represent Monte Carlo statistical errors. The impact of p_t uncertainty is a factor of three less in the Hadronic Hose case, and below 8 GeV the Hadronic Hose beamline shows no significant variation at all.

2.3 Hadron Production Model Uncertainty

The calculation of the neutrino flux is roughly 20% uncertain due to a lack of precise knowledge of the hadron production spectrum from the target.

As exemplified by Figure 5, the hadronic production as a function of p and p_t is not well measured at energies of $\sim$ 100 GeV. Further, to calculate rates for NuMI targeting from this data set involves (i) an extrapolation from the hydrogen target measurements to a thick carbon target, (ii) an extrapolation in beam energy to 120 GeV protons, and (iii) interpolation and extrapolation to x and p_t ranges that were not measured.

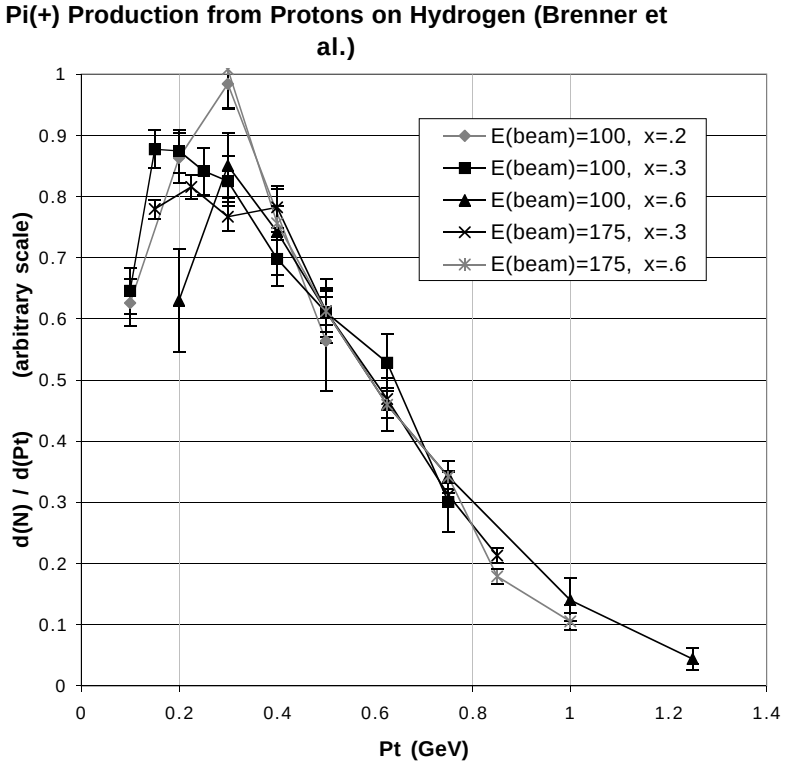

Figure 5: Hadron p_t distributions from data taken by Brenner *et al.* [2].

Given the measurement of a neutrino energy spectrum in the near detector, one could tune the x distribution of pion production in the Monte Carlo to reproduce it. One could then extrapolate the neutrino flux from the near detector to the far detector. The systematic uncertainty in the Monte Carlo extrapolation from near to far could be estimated by studying the result of reasonable variations of the p_t spectrum.

Recent measurements from the SPY collaboration, where p_t scans were made at two x values for protons on Beryllium, show significant variation of the p_t shape with x (Figure 6). This illustrates a problem with the WANG model [3], the CKP model [4], and the Malensek model [5], where a universal p_t shape is assumed. Even more modern models such as FLUKA only claim to reproduce the distributions to 20% [6].

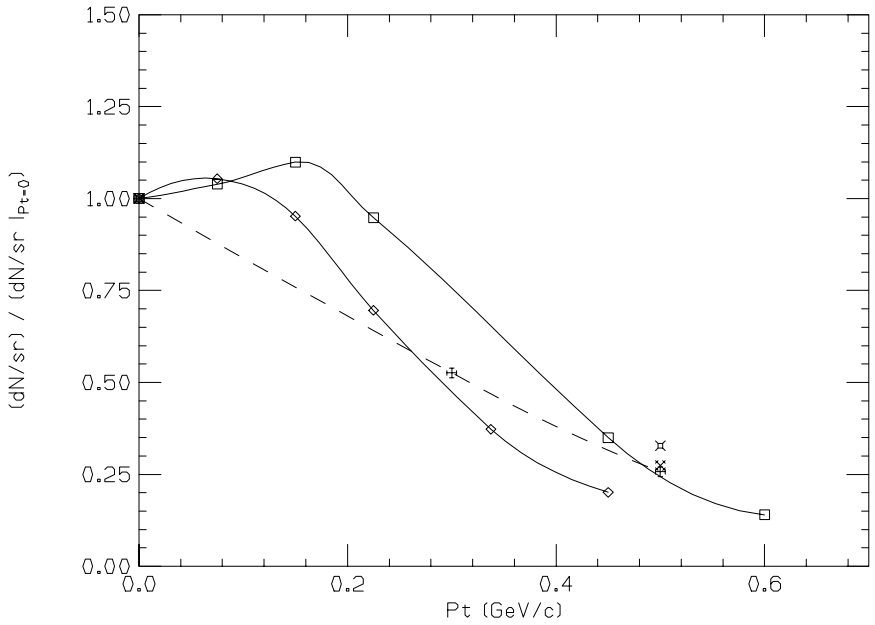

Figure 6: p_t distributions, N_{π^+}/steradian, normalized to 1 at p_t=0. Solid curves are from data taken by the SPY collaboration using 450 GeV protons on a Be target [7]. The two curves are from logitudinal momenta of 15 GeV/c and 40 GeV/c. The stand-alone points and the dashed curve are from data taken by Atherton [8] using 400 GeV protons; the dashes are not meant to represent the real shape of the spectrum but just join the data points.

Figure 7 shows a variation of the `GEANT/FLUKA` model which changes $\langle p_t \rangle$ from 0.37 GeV to 0.55 GeV. This is adequate to cover the $\langle p_t \rangle$ range found in other models of hadron production (e.g., WANG [3] has $\langle p_t \rangle$=0.42 GeV, the CKP model [4] has $\langle p_t \rangle$=0.44 GeV, and the Malensek model [5] has $\langle p_t \rangle$=0.50 GeV), although it does not address variations of the p_t shape with x. Figure 8 shows the relative changes in the near and far spectra as such a variation is made. Figure 4 shows the fractional change in the far-near ratio under this variation of the p_t spectrum for PH2ME and with the addition of the Hadronic Hose. While more sophisticated studies are planned, they will take some time.

The fact that the change induced in the near spectrum is somewhat different

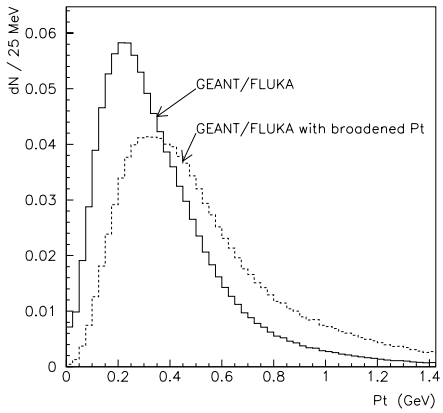

Figure 7: Pion p_t production distributions propagated through the `GNuMI` Monte Carlo to study hadronic production systematics. The distributions used are momentum dependent; these are the average over all momenta.

from that induced in the far detector demonstrates that the variations in p_t induce a systematic uncertainty in the extrapolation from the near detector spectrum to the far detector. This uncertainty from the hadronic production model is likely to be the limiting systematic error for the ν_μ CC Total Energy oscillation test unless one or both of the following options are taken:

- Measure the hadronic production spectrum from a carbon target with 120 GeV protons. This involves a separate fixed target experiment. The production rates in p and p_t would need to be measured to a few percent.
- Implement continuous focusing in the decay pipe, i.e. the Hadronic Hose.

2.4 Effect on Horn Tolerances

In general, mechanical tolerances are eased by the Hadronic Hose, as illustrated in Table 1. For instance, the effect of an induced field in the central hole of the horn due to thickness variations in the inner conductor (which is perhaps the hardest tolerance to meet that we know of) is reduced so that the tolerance is a factor of two less stringent compared to the baseline configuration.

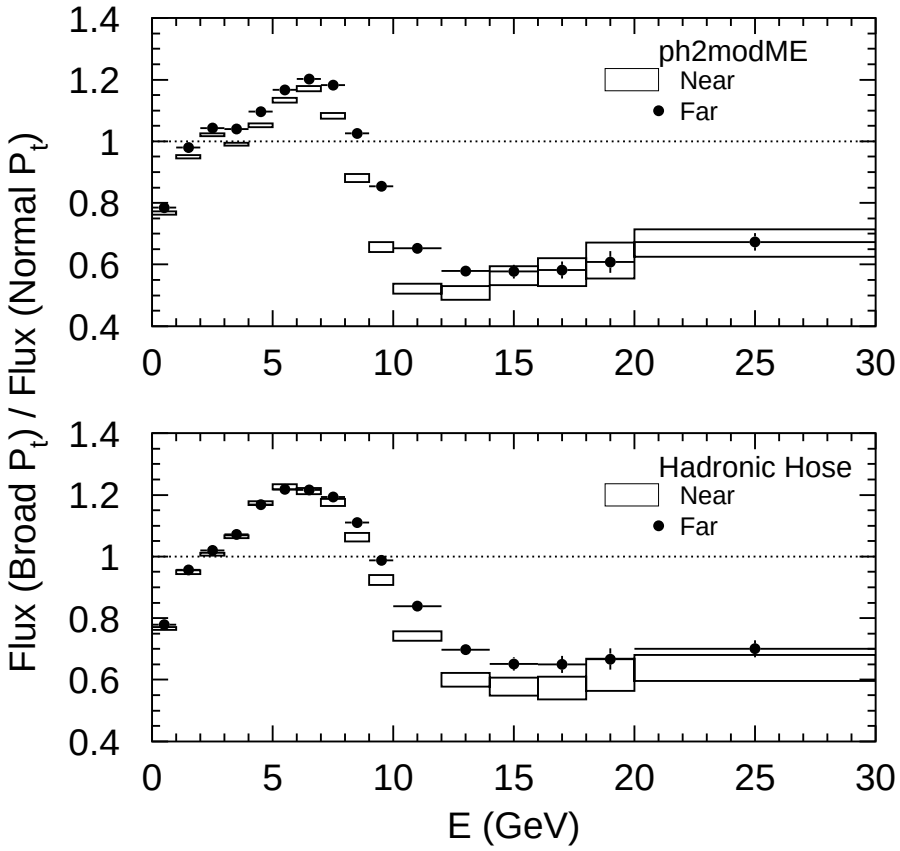

Figure 8: Relative change in the near and far detector spectra assuming a broadened hadron production p_t spectrum. Top figure is for the baseline PH2ME beam and bottom is with hadronic hose added.

Horn design tolerance	ME beam		LE beam	
	w/o HH	HH	w/o HH	HH
Constant along the length eccentricity of the inner conductor in horn#1	0.035 mm	0.065 mm	0.08 mm	0.10 mm
Axis shift (misalignment) of horn#1	0.5 mm	0.8 mm	0.8 mm	1.0 mm
Current variation in horns	±0.6%	-2.5% +1.5%	±1.0%	-1.7% +1.2%

Table 1: The effects of Hadronic Hose with I=1.0 kA on some of the most important tolerances for the PH2 Horn focusing system. Tolerances given provide ≤2% deviation of the FAR/NEAR ratio from its nominal values in the neutrino energy range of 0-18 GeV.

2.5 M.C. Independent Prediction of Far Spectrum from Near

One interesting characteristic of the Hadronic Hose beam is that prediction of the far spectrum from the near can be done to the 10% level without the use of any Monte Carlo, whereas with the baseline PH2ME design a Monte Carlo is required to get any sensitivity to neutrino oscillations.

2.5.1 Idealized $1/R^2$

The ideal neutrino source would be a point source. Then defining R_F to be the distance to the far detector and R_N the distance to the near, and $Flux_{Far}(E_\nu)$ to be the flux in the far detector as a function of E_ν,

$$Flux_{Far}(E_\nu) = (\frac{R_N}{R_F})^2 \; Flux_{Near}(E_\nu)$$

But NuMI is an extended source, with distance from target to end of decay pipe being about 720 m, while the distance from the end of the decay pipe to the MINOS near detector is only about 320 m.

2.5.2 Baseline PH2ME

The basic way to use the near detector information to predict the far spectrum is to scale the Monte Carlo prediction

$$Flux_{Far}(E_\nu) = \frac{M.C._{Far}(E_\nu)}{M.C._{Near}(E_\nu)}\ Flux_{Near}(E_\nu)$$

This is nearly as well as one can do, given the degrees of freedom in hadronic production, and is used as the model for calculations of systematics in this proposal.

2.5.3 Hadronic Hose

Let us take the simplest extended source model we can imagine. Start with the idealized $\frac{1}{R^2}$ model above, but integrate it over the length of the decay pipe weighted by the pion decay lifetime which corresponds to the neutrino energy $E_{\nu_\mu} = 0.43E_\pi$

$$Flux_{Far}(E_\nu) = \frac{\int_{48\ m}^{720\ m} \frac{e^{-\frac{0.43 m_\pi z}{E_\nu c\tau}}}{(R_N - z)^2} dz}{\int_{48\ m}^{720\ m} \frac{e^{-\frac{0.43 m_\pi z}{E_\nu c\tau}}}{(R_F - z)^2} dz}\ Flux_{Near}(E_\nu) \qquad (1)$$

This treatment ignores many things: decay angles, Kaons, secondary interactions, the tail of π decays to neutrino energies lower than $0.43E_\pi$, etc., but works surprisingly well in the Hadronic Hose case in the region of interest, as shown in Figure 9.

2.6 ν Event Rates

The event rate as a function of Hadronic Hose current is shown in Figure 10. (A year for NuMI is conventionally taken as 3.8×10^{20} protons on target). For the Medium Energy beam configuration, the Hadronic Hose gives a modest increase in the event rate compared to the baseline beam. For the Low Energy beam configuration, the increase in event rate for 1 kA is around 27%. This is a significant improvement, especially since this is the beam configuration is sensitive to the lowest Δm^2 regions and is statistics limited. While the Hadronic Hose cost has not been estimated very precisely, it appears small compared to e.g. the cost of additional detector mass or decay pipe radius to achieve the same increase in rate.

For resonant extraction, the hose current is limited to about 1 kA. For single turn extraction a higher current should be possible (although at increased cost

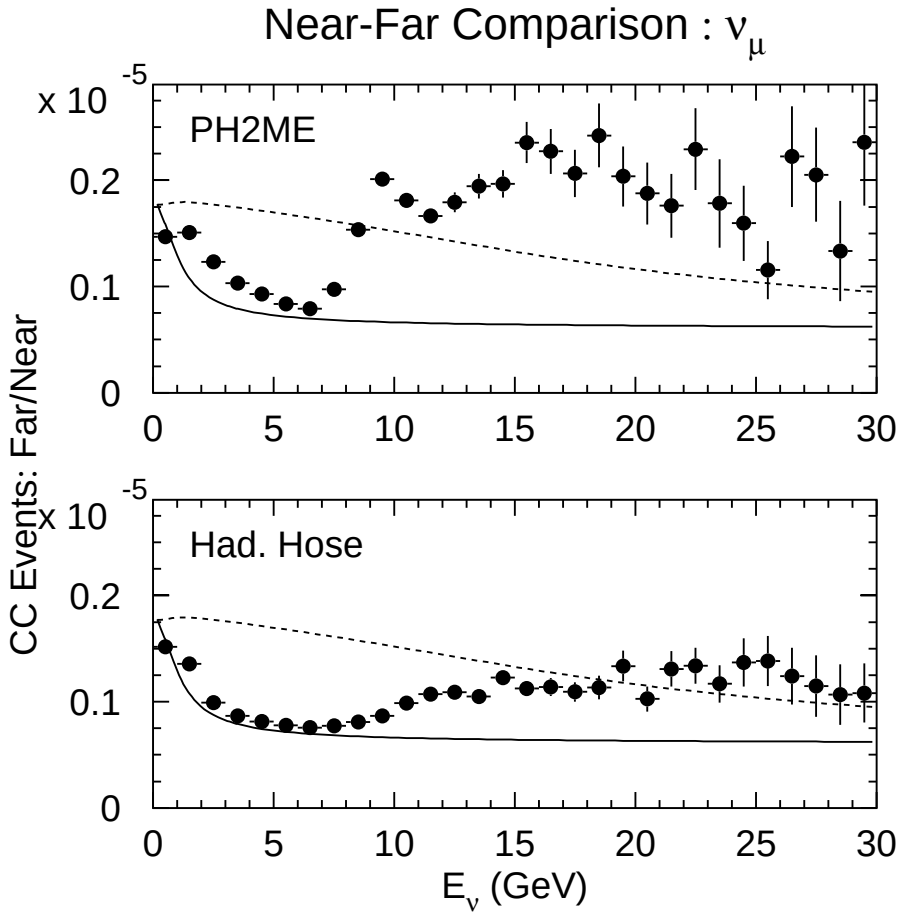

Figure 9: The ratio of the far to near spectrum for PH2ME (top) and for PH2ME with the addition of the Hadronic Hose (bottom). In each plot the solid curve is the expected ratio based on the pion lifetime and the dashed curve is the expected ratio based on the Kaon lifetime.

for the power supply). This would be desirable to achieve the highest event rate for low energy beam.

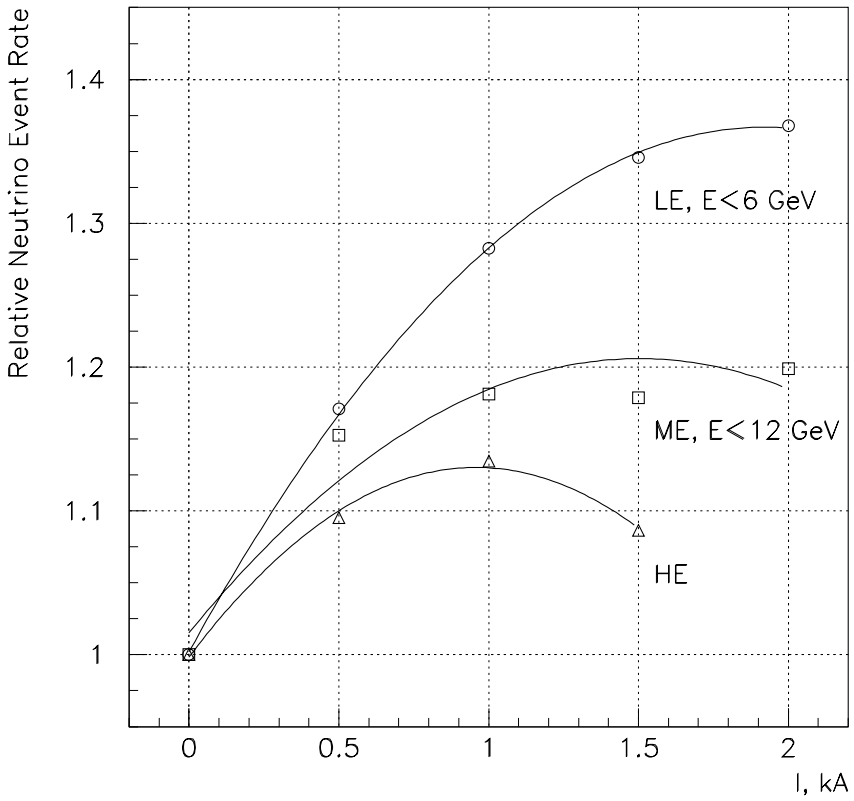

Figure 10: The ν_μ CC event rates in the far detector as a functions of the Hadronic Hose current and the PH2 horn beam configuration.

3 Hadronic Hose Design Parameter List

Parameter	Baseline	Alternate
Radius, thickness of decay pipe	1 m, 13 mm	
Wire radius	1.2 mm	1.0 - 1.4 mm
Wire material	Al EC-H18	(see Appendix B)
Number of segments	60	
Length of segment	11 m	
Gap between segments	0.1 m	
Expansion of a segment 20°C to 188°C	0.03 m	
Start distance from 1st horn	50 m	
Distance between wire supports	2.2 m	
Current	1000 Amps	700 Amps
Pulse ramp up	$\sim$ 0.5 ms	
Pulse flattop	1 ms	10 μsec
Wire resistive voltage drop per segment	104 Volt	
Inductance per segment	15×10^{-6} henry	
End crimp length, radius	25.4 mm, 3 mm	
Vacuum	1 torr	0.01 - 10 torr
Temperature jump from i^2r heating	1.1° C	
Temp. jump from beam heating	0.9° C	
Emissivity of anodized wire	0.7	
Heat trans. coef. residual gas	1.7 w/m^2/K	
Wire temperature	188° C	
Decay pipe temperature	50° C	
Wire segment expansion per pulse	0.4 mm	
Tension on wire	9 lbs	
Stress from pretension	1300 psi	
Sag of wire	$\pm$1 mm	
Alignment tolerance	2 mm	

Table 2: Set of Hose design parameters, with possible design variations.

4 Hadronic Hose Simulations

4.1 Description of Monte Carlo Simulation

The performance of the Hadronic Hose has been modeled through a series of GEANT simulations. The geometry of the hose used in the simulations is diagrammed in Figure 11. The simulation uses 60 segments of Hadronic Hose wire each separated by a 10 cm gap. The segments are 11 m long and include a 1.4 mm radius aluminum wire running down the beam axis with lead and return wires running out to the decay pipe wall along the x-axis at each end. This wire is supported at each end by three 1 mm diameter aluminum wires running out to the decay pipe walls. The support wires are positioned at angles of $\phi = 0^\circ$, 120° and 240° and are angled at 45° with respect to the beam axis to provide tension on the central current wire. Aluminum connectors 6 mm in diameter and 26 mm long are included at each end of the current wire. The wire is supported at four additional locations along its length by similar sets of three wires, but which are perpendicular to the beam axis instead of angled at 45°. The calculation of the magnetic field assumes a uniform current of 1 kA but includes the effects of the lead and return wires as well as the gap between segments.

4.2 Comparison With Baseline PH2 Medium Energy Beam

Figure 1 shows the expected ν_μ charged-current events rates for the baseline two horn, medium energy beam (PH2ME) and for the baseline design with the addition of the Hadronic Hose. The broader Hose spectrum may be moderately more attractive for searching for oscillation signals over a range of Δm^2. The additional focusing from the Hadronic Hose increases the far detector event rate by around 18% over the baseline beam design. As mentioned in previous sections, it improves the far-near spectrum comparison, and as shown in Figure 9 makes the far-near ratio close to the expectation based on the pion lifetime.

Figure 12 shows the fractional content of the neutrino beam as a function of energy for the baseline PH2ME beam and with the addition of the Hadronic Hose. The Hadronic Hose defocuses negatively charged mesons, reducing the content of ν_μ significantly above 10 GeV. The addition of focusing of muons increases the ν_e content roughly from 0.5% to 0.8%. Figure 13 plots the expected ν_e charged-current spectrum for the PH2ME beam with and with out the Hadronic Hose.

The effects of variations in the hadronic p_t spectrum on the ν_μ CC event spectra were studied for the baseline PH2ME design and for the design including

Hadronic Hose

→ Current carrying wire running down center of decay pipe

→ Provides continuous focusing of π's and K's

60 Sections each 11 m long

Current = 1 kA, B = 0.02 kG at r=10 cm

Aluminum wire, r ≥ 1 mm, T = 170^{o} C

For each section ΔV = 170 Volts

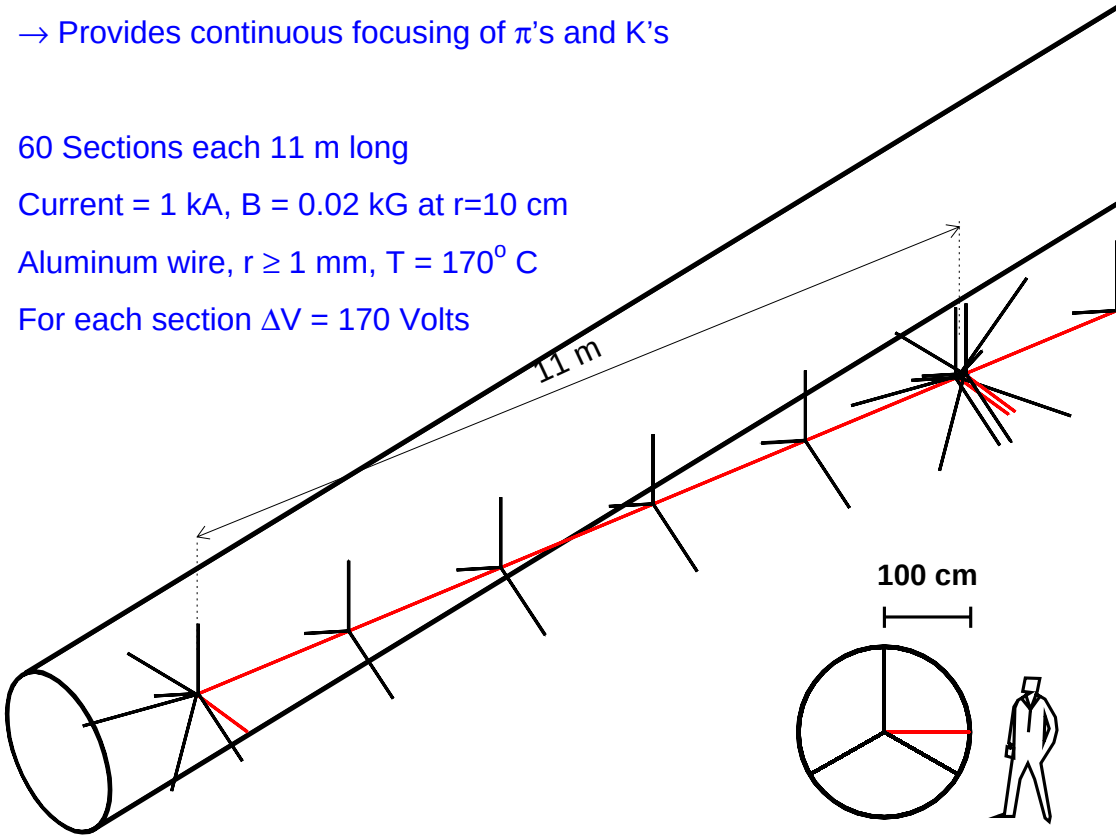

Figure 11: A schematic drawing of the Hadronic Hose as implemented in the GEANT simulations.

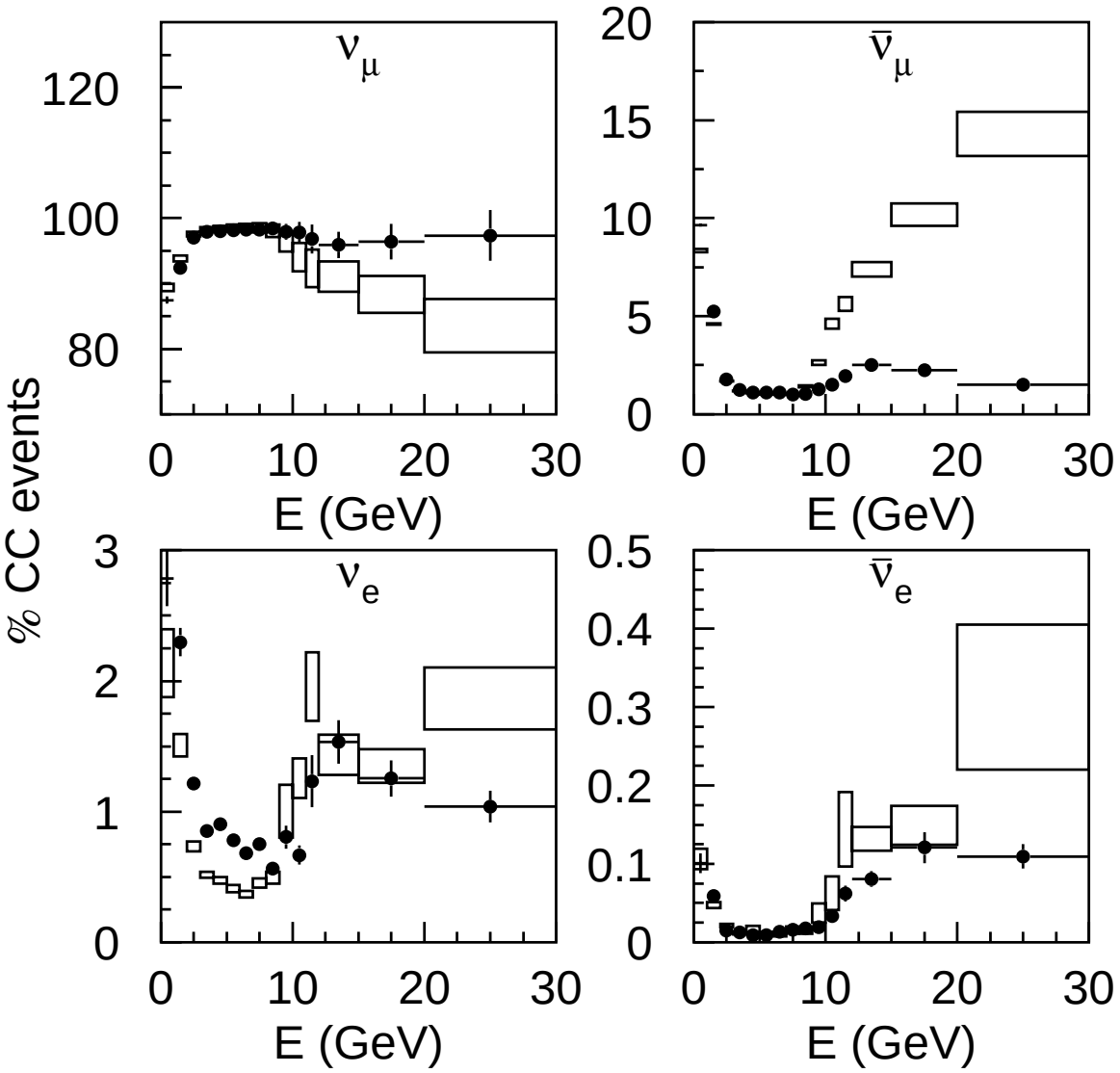

Figure 12: The fractional composition of the neutrino beam is plotted as a function of energy for the baseline PH2ME beam line (boxes) and with the addition of the Hadronic Hose (points). With the addition of the Hadronic Hose, the fractional content of ν_e in the beam increases from roughly 0.4–0.5% to 0.7–0.8% in the range from 2–10 GeV.

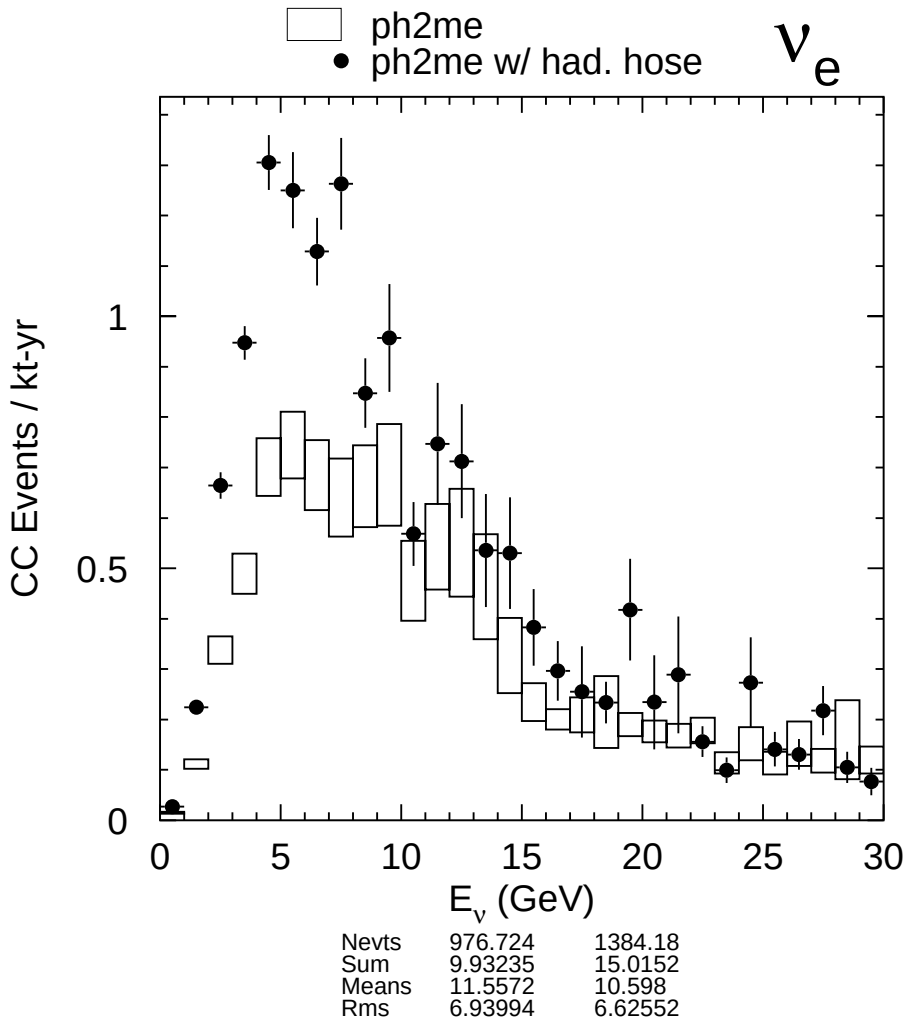

Figure 13: Comparison of the expected ν_e charged-current event rates for the baseline medium energy beam (boxes) and the baseline with the addition of Hadronic Hose (points).

Hadronic Hose. The ratios of the near and far ν_μ CC event spectra are plotted in Figure 8 for a nominal (`GEANT-FLUKA`, $\langle p_t \rangle = 0.37\ GeV$) p_t spectrum and for a broadened p_t spectrum ($\langle p_t \rangle = 0.55\ GeV$). The effect of broadening the p_t spectrum on the far/near ratio is plotted in Figure 4. The largest variation in the far-near comparison under this broadening of the p_t spectrum is 35%; with Hadronic Hose the largest variation is 18%, although these are not in the neutrino energy region of interest. Below 8 GeV the baseline design shows an oscillation-like 5% wiggle while for the Hadronic Hose design no significant variation is observed.

4.3 Choice of Wire Material

To study the effects of wire material, simulations were made using no wire material, as well as aluminum, copper and tungsten. The CC event spectrum at the far detector using no wire material and aluminum wire are compared in Figure 14. The addition of the material results in a 3-6% decrease in the event rate below 10 GeV. Higher energies are not affectes. Rates of ν_e are also not affected significantly. Figure 15 shows the change in the ν_μ CC event rate at the far detector as a function of the atomic number of the wire material. In each case the wire radius was 1.4 mm. As much as a 9% decrease in the event rate below 12 GeV is seen for the highest Z material. Decreases for the highest energies (above 12 GeV) are larger; almost 15%.

The change in event rate is plotted in Figure 16 as a function of wire radius. In the figure, the event rates are compared to simulations using no wire material. All simulations used aluminum wire. The event rate below 6 GeV is most strongly affacted by the wire radius with roughly a 5% decrease a a radius of 1.4 mm. The difference in rate between 1 mm radius wire and 1.4 mm radius wire is at most 2%.

4.4 Alignment Tolerance

The effect of misalignment of the Hadronic Hose wire was tested by introducing random displacements of the wire ends in (x, y and z). The displacements were Gaussian distributed with zero mean and and rms of between 0 and 10 mm. Variations in the locations of the wire ends were uncorrelated resulting in a random misalignment of each segment of hose wire with respect to the beam axis. The calculation of the resulting magnetic field accounted for the misaligned wire positions.

The relative event rates are plotted in Fig 17 as a function of the rms misalignment. In these simulations, a 1.4 mm radius aluminum wire was used.

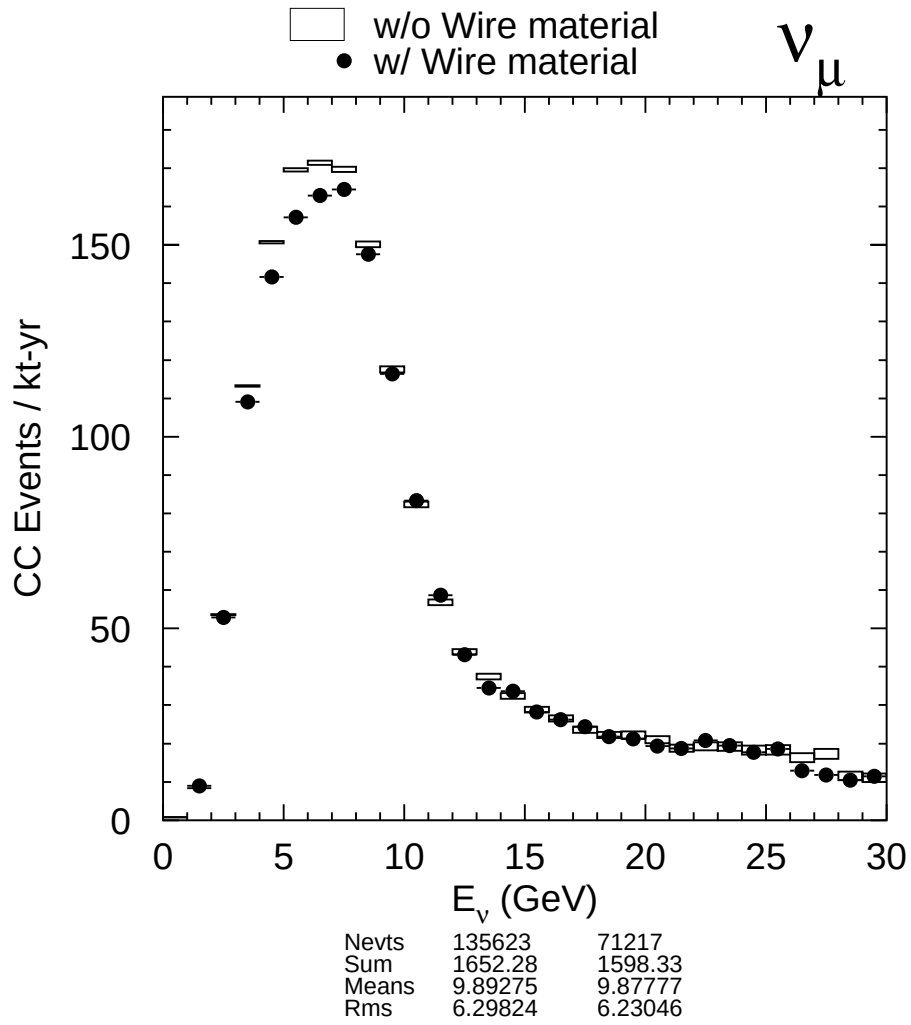

Figure 14: Comparison of the ν_μ charged-current event spectrum for the PH2 medium energy beam with Hadronic Hose. Simulations with aluminum wire material (points) and without wire material (boxes) are compared.

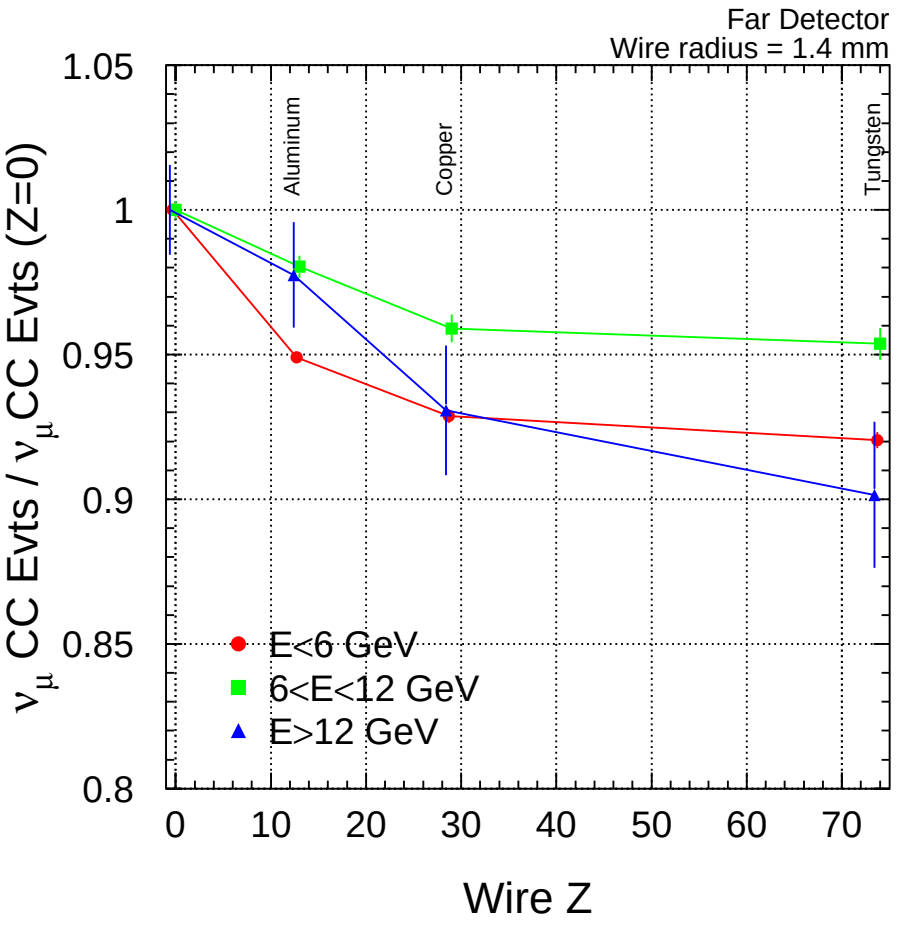

Figure 15: The relative far detector event rate in three energy regions as a function of wire material.

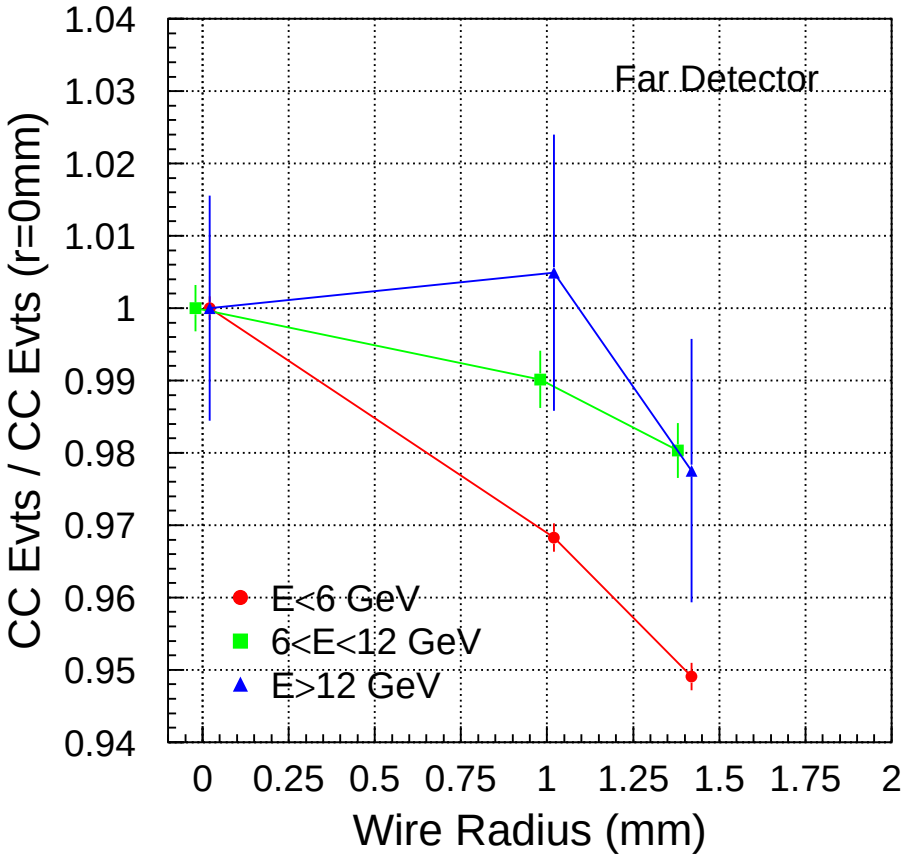

Figure 16: The relative far detector event rate in three energy regions as a function of wire radius. In each case, aluminum was used as the wire material. For the purposes of cooling, the wire radius must be kept between 1 and 1.4 mm.

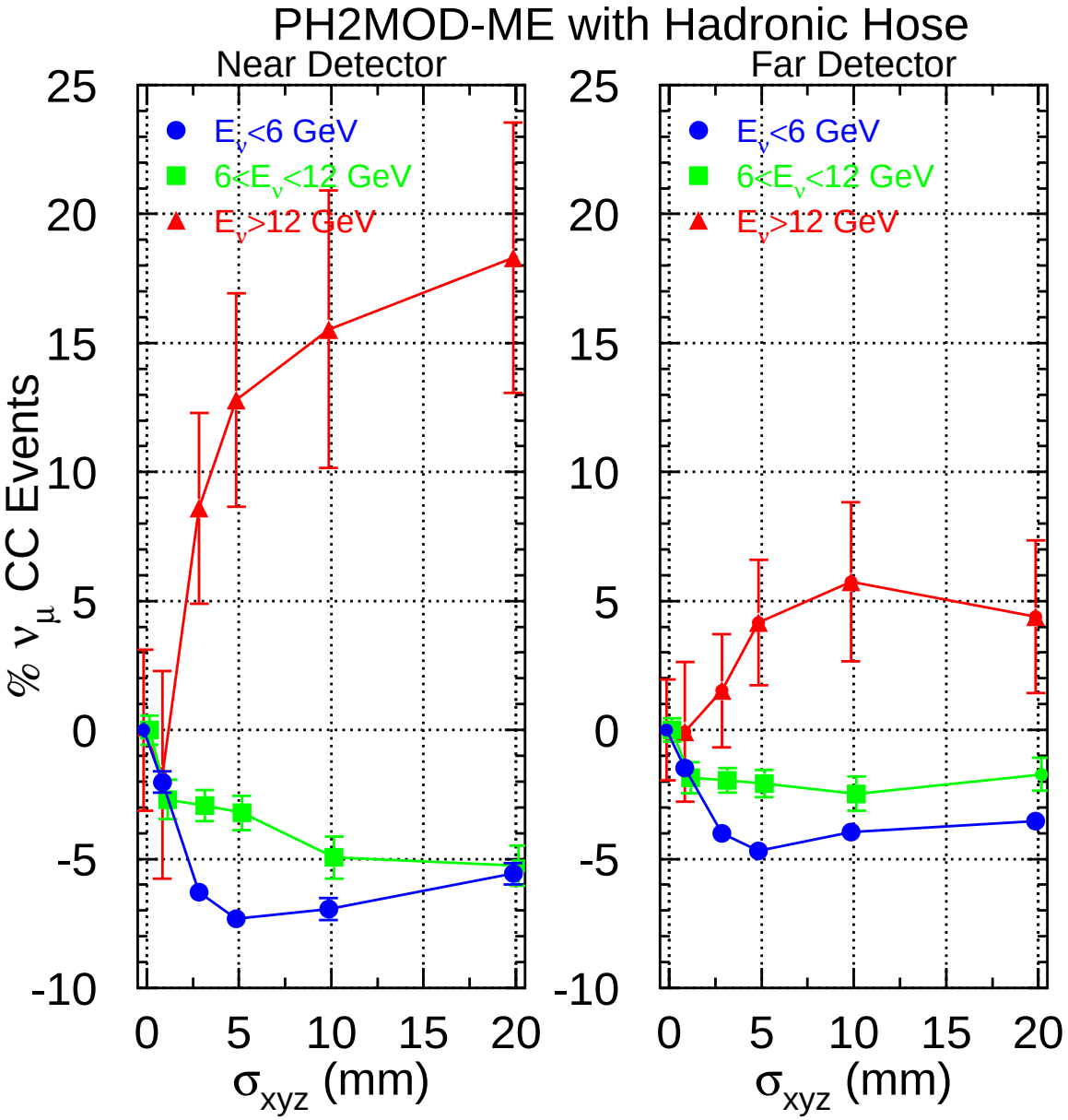

Figure 17: The relative event rates at the near and far detector are plotted as a function of the *rms* mis-alignment of the Hadronic Hose wires.

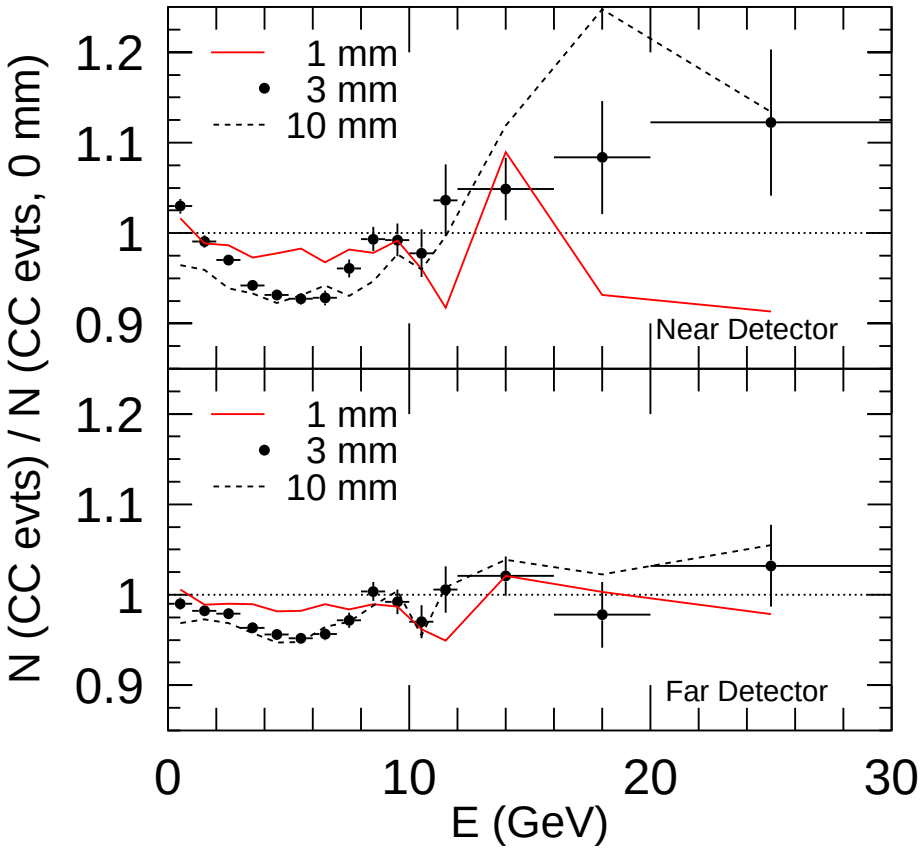

Figure 18: Comparison of the near and far detector ν_μ charged-current event rates for a misaligned hose relative to a perfectly aligned hose.

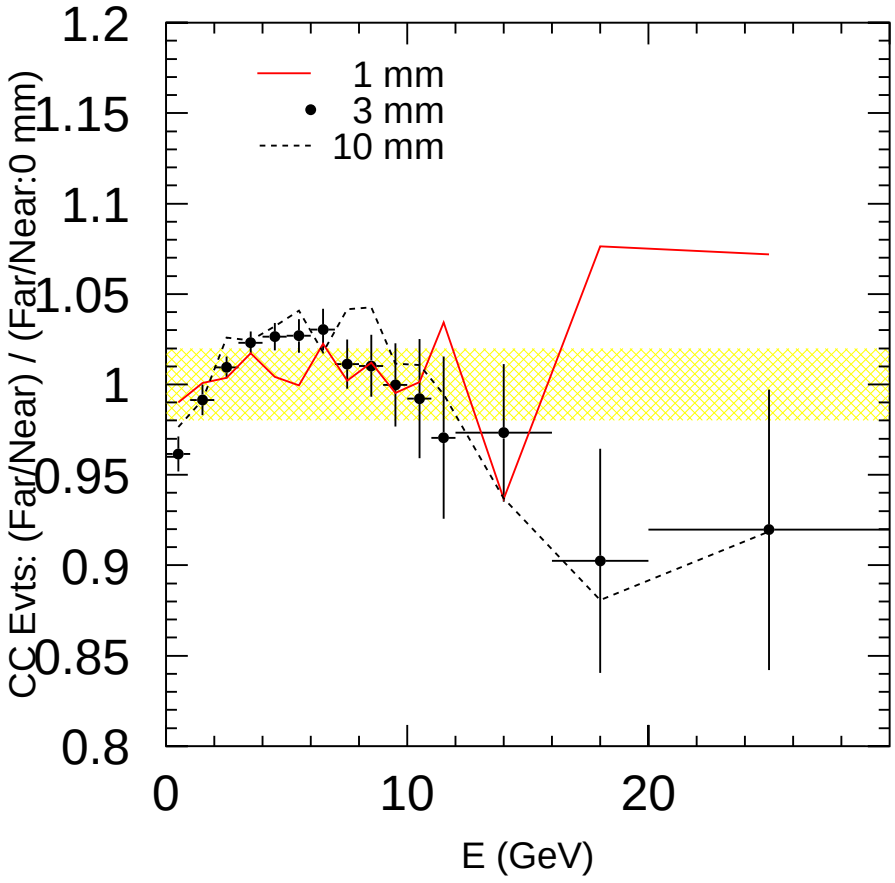

Figure 19: Comparison of the far-near ν_μ charged-current event double ratio for a perfectly aligned Hadronic Hose and a hose with random misalignments. The shaded band is $\pm$ 2%.

At low energies mis-alignment results in roughly a 3-7% decrease in the event rate at the near detector and a 2-5% decrease in the event rate at the far detector. Mis-alignment results in a relative increase in the high energy neutrino event rate.

The relative ν_μ charged-current spectrum for the aligned and misaligned Hadronic Hose cases are plotted in Figure 18. Misalignment of 3 mm results in approximately a 1-5% decrease in the event rate at the far detector below 8 GeV. The resulting deviations in the far-near detector ratios are plotted in Figure 19. Below 10 GeV, where the event rate is largest, the deviations introduced by 3 mm misalignments are within 2.5%, suggesting that alignment tolerances of somewhat less than 3 mm would be acceptable.

4.5 Segment Failure

The performace of the Hadronic Hose has been simulated under various failure conditions. In the first study, a hopefully pessimistic failure rate of 10% of the wire segments was assumed. Of the 60 segments, segments 7, 26, 30, 35, 53 and 58 were randomly selected to be turned off. The resulting CC ν_μ spectra for the near and far detectors are plotted in Figure 20. This failure rate causes roughly a 10% decrease in the near and far detector events rates. The effect on the far-near comparison is shown in Figure 21. This failure rate causes roughly a 3% variation in the far-near ratio which does not depend significantly on energy. Segment failures would be monitored and presumably could be input to the simulations.

Simulations were also made assuming failure of the first two segments. As these segments receive the most beam heating they are perhaps more likely to fail. The resulting relative far detector ν_μ spectrum is shown in Figure 22. Failure of the first two segments results in roughly a 3% decrease in the event rate below 8 GeV. The largest decrease is 10% between 10 and 12 GeV. Figure 23 shows the resulting change in the far-near ratio. All variations below 8 GeV are within 2%.

4.6 Further Monte Carlo Needs

The main Monte Carlo issues remaining have to do with possible variations in Hadronic Hose design to allow reduction in the temperature of the wire where beam heating is worst. One should check the impact of lower overall hose current for the Medium Energy beam, and the impact if front sections were run at lower current.

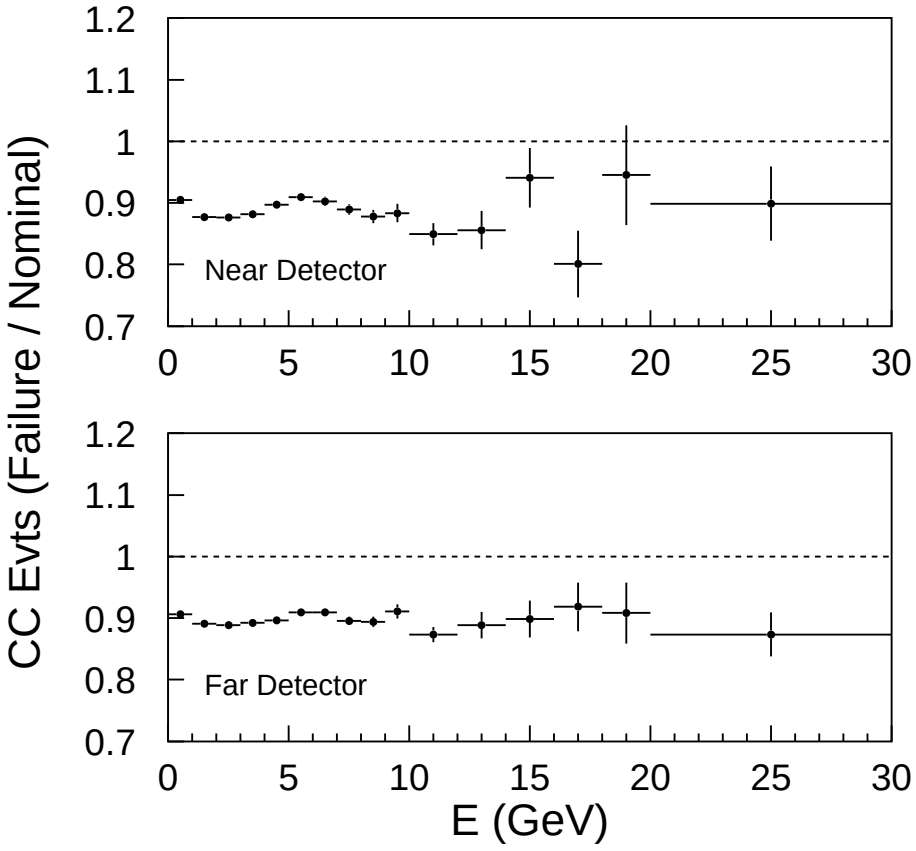

Figure 20: The relative spectra for the near and far detectors for a simulated 10% Hadronic Hose segment failure compared to a fully operational Hadronic Hose.

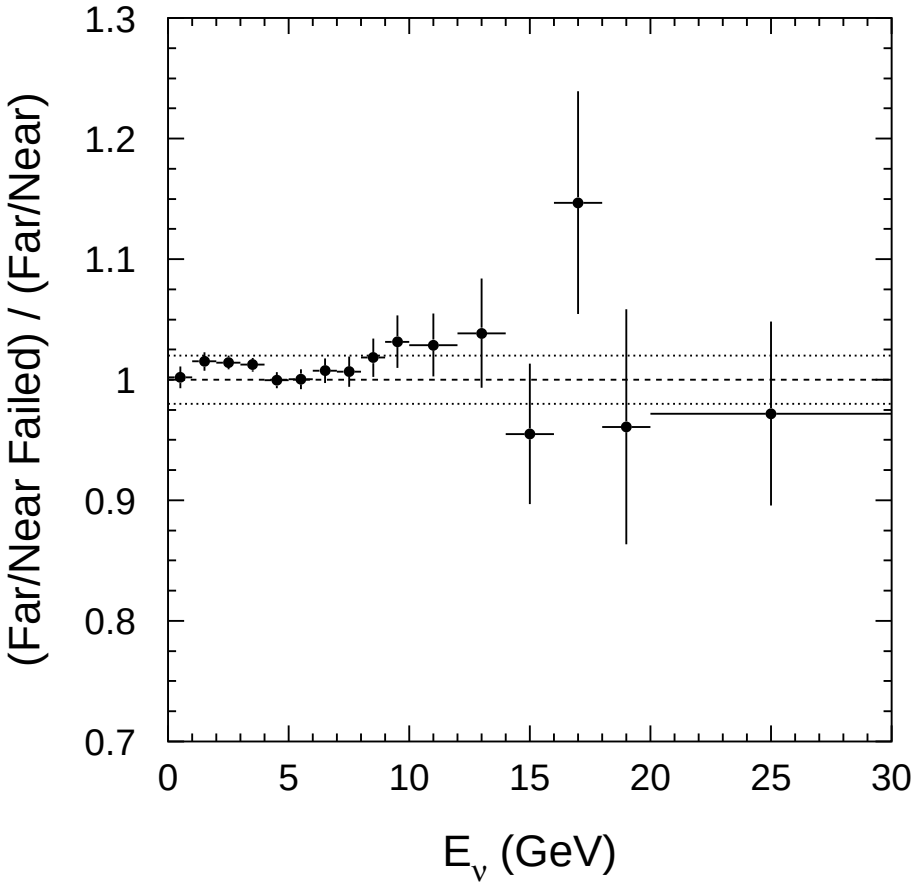

Figure 21: The variation in the far-near ratio is plotted assuming a 10% segment failure rate. Variations in the far-near ratio are roughly flat and within 3% below 10 GeV.

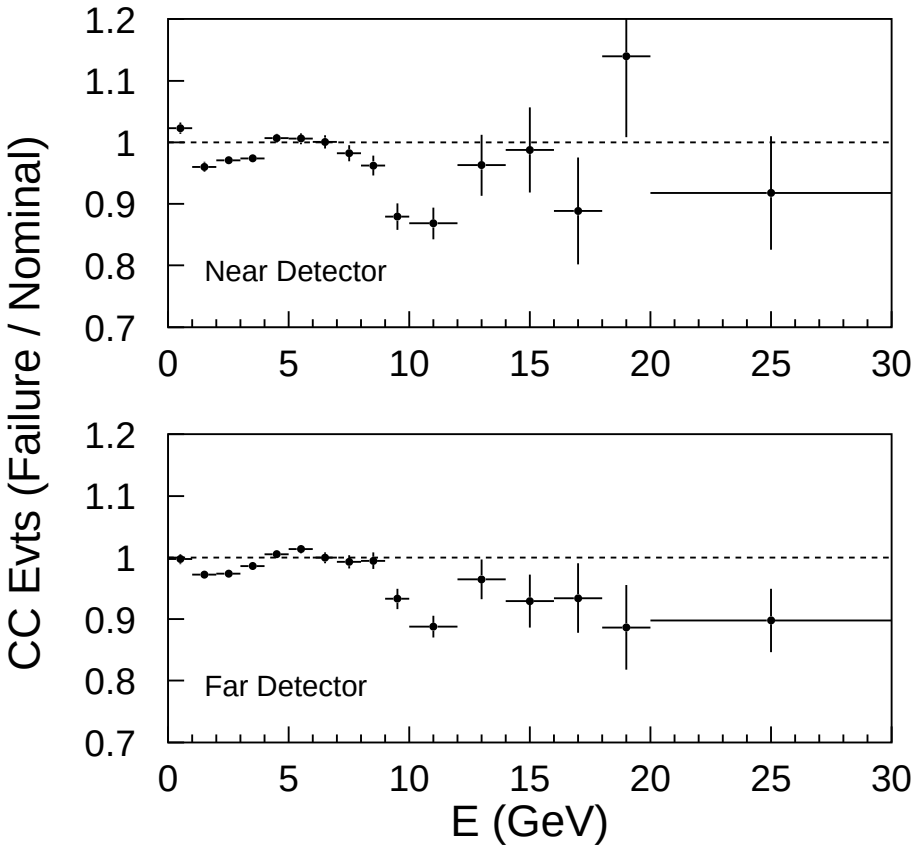

Figure 22: The relative spectra for the near and far detectors with a simulated failure of the first two of sixty Hadronic Hose segments.

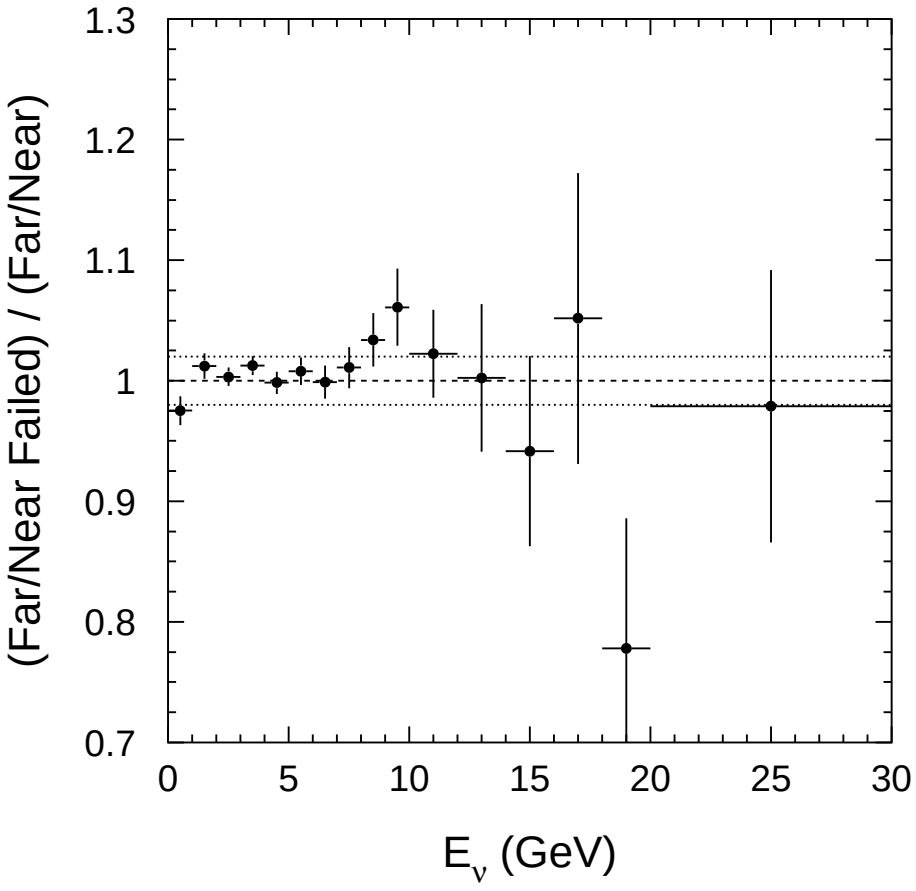

Figure 23: The change in the far-near ratio assuming a failure of the first two Hadronic Hose segments relative to a fully operational hose.

Also, most of the Monte Carlo has been done with Medium Energy beam, and some of these studies should be repeated with Low Energy beam.

5 Hardware Issues

An R&D program is currently underway to study the problems of wire cooling, creep, vibration, and long term mechanical stability.

Probably the hardest technical challenge is to radiate enough heat from the wire, while still carrying sufficient current. Aids to accomplishing this are to pulse the current only during the beam spill, and to anodize the wire to improve heat loss by radiation. Making the 'wire' in the form of tubing and flowing water through it to actively cool it is another possibility that appears to be technically feasible (that is, tubing size, required water pressure, and resulting temperature are all reasonable), but is a complication to the design that one would not assume lightly.

A test stand has been assembled with a 3.5 m long wire installed in a 6 inch vacuum beam pipe. A power supply was built that can produce a sinusoidal current pulse on the wire with 2.5 ms baseline and 840 Amp peak. Other tests were carried out with a 20 Amp D.C. power supply. One end of the wire is fixed, the other end is spring tensioned. A mark on the spring tensioned end of the wire is viewed with an optical survey instrument through a window to both measure creep and to measure wire expansion with temperature.

5.1 Wire Radius and Heating

Aluminum wire EC H18 was selected because it has good conductivity (which reduces heating), and can withstand reasonable tension. (See Appendix B for some other possible wire materials). Aluminum has fairly low density, which helps to reduce beam heating, and may reduce absorption of pions. It is easily available, and can be anodized readily. Higher strength means the possibility to use higher tension, which translates to fewer supports to maintain small sag.

Anodized wire has been compared to non-anodized wire in the Hadronic Hose test stand. Further refinement of the measurement technique is needed, but the emissivity increased from about 0.1 for shiny wire to about 0.7 for anodized wire.

The larger the wire, the smaller the electrical heating of the wire; however, the size of the wire is limited by two factors. First, a noticeable fraction of the pions orbiting the wire will be absorbed if the wire radius is $\sim$2 mm or larger. Second, larger wires experience greater beam heating as the heat absorbed by the

wire increases as the volume while the heat radiated increases only as the surface area. The temperature of a wire segment at the beginning of the decay pipe is plotted in Figure 24 as a function of wire radius. The minimum possible wire temperature is obtained for radii in the range of 1.0 to 1.6 mm (see Figure 24).

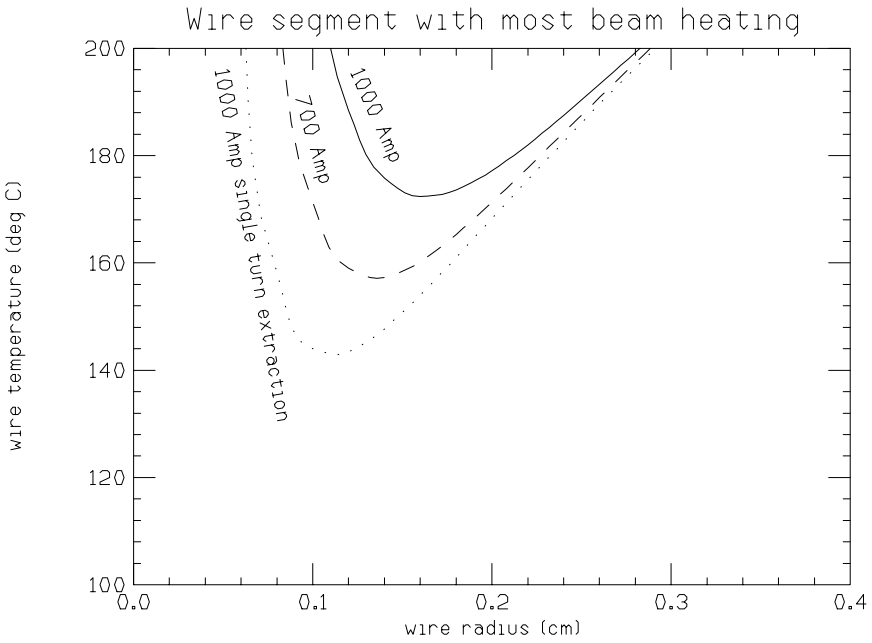

Figure 24: Temperature of the wire as a function of design radius. Calculated at the beginning of the decay pipe, where beam heating is largest. If single turn extraction of the beam is adopted, then a reduction in the pulse length can be made, resulting in the dotted curve.

The temperatures shown in Figure 24 correspond to values extrapolated from preliminary data taken with the Hose test stand. Beam heating is estimated using the CASIM Monte Carlo[9]. The number given corresponds to a point after the first few meters of wire, 0.86 Joule/gram/spill. The scaling with temperature of the cooling due to residual gas is not fully understood, so the shape of the curves may still change. The rate of cooling has, however, been tested with wire and pipe at their expected design temperatures (see Appendix C).

The MARS Monte Carlo has been run with the PH2me design of target, horn, decay pipe, and Hadronic Hose wire to give an independent estimate of beam heating. The initial run gave an energy deposition in the wire two orders of magnitude below the CASIM result.

Since we have not found the problem in either Monte Carlo yet, three other methods have been used to get a handle on the beam heating. The first is to get a rough lower bound by taking the 13% of protons that are left after

two interaction lengths of target, spreading them out by the 0.24 milliradian coulomb scattering occuring in the target, and multiplying by dE/dx—$_{min}$ of 1.62 MeV cm^2/g in Aluminum to get 0.16 Joule/gram/spill. This can be compared to 0.86 Joule/gram/spill from CASIM and 0.01 Joule/gram/spill from the MARS. This would seem to indicate a problem with our understanding of the MARS Monte Carlo.

As a second step, a simple MARS run was done firing 120 GeV protons into an Aluminum wire without magnetic field. Taking the peak energy deposition, which occured about 12 cm into the wire, and multiplying by the flux of protons estimated in the first method gives 0.32 Joule/gram/spill.

In the third method, the particle density just before the wire was taken from the GNUMI Monte Carlo. This flux was $28 \times 10^9/mm^2$, compared to $6 \times 10^9/mm^2$ for the uninteracted proton estimate above. If all these particles gave energy deposition like protons in the simple MARS run, then the energy deposition would be 1.5 Joule/gram/spill at the MARS shower maximum, while CASIM gives 2.4 Joule/gram/spill at the same location.

The general conclusion is that the original CASIM result appears not unreasonable, and the full simulation in the MARS Monte Carlo needs further work.

The beam heating decreases down the rest of the Hose. Special care may well have to be taken with the first section. Three good possibilities are: (i) With the addition of more supports for the first section, the wire sag can be acceptable even with zero external tension. (ii) For PH2le and PH2me, the first hose section could be in the helium-filled beam-transport pipe in the target hall instead of in the vacuum decay pipe. Helium is an excellent cooling gas. (iii) That section can be run at reduced current.

Understanding the full MARS simulation, and extending it to include e.g. hose misalignment, should be a high priority task.

5.2 Voltage breakdown

The breakdown voltage was measured with the Hadronic Hose test stand as a function of the vacuum level. The results shown in Figure 25 are in general agreement with theoretical expectations, and indicate that anything over 375 V would not be safe. This is another reason that the Hose wire must be made in sections, where the voltage on each section can be kept low. Setting a goal of keeping the maximum voltage in the decay pipe to around 200 V gives a large safety margin.

With the standard parameter list, the wire resistive voltage drop in a segment is about 100 Volts. Assuming a ramp to flat-top of order 0.5 milli-seconds,

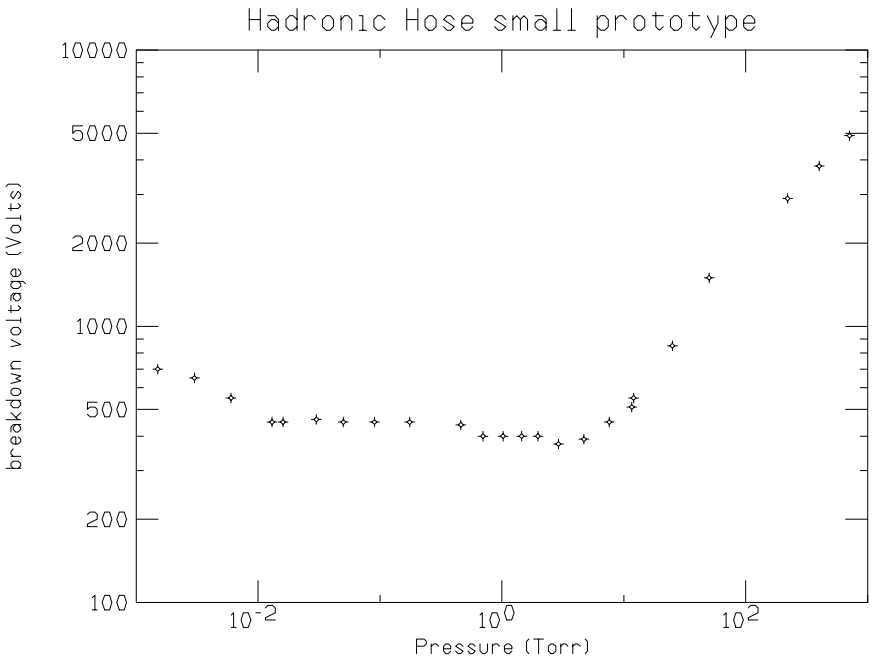

Figure 25: Breakdown voltage in Hadronic Hose test stand as a function of vacuum level.

the inductive voltage $V = L\ dI/dt$ is 30 V for an 11 m segment. Using the above criterion, a segment could be twice as long as in the base Hose parameter list, or the wire resistance could be twice as high, and still maintain a good safety factor. Also, the ramp-to-flattop could be considerably faster.

5.3 Wire Vibration

The wire in the Hose test stand was observed through a glass window when the current was pulsed, and wire vibration was seen to be less than 1 mm. This test should be repeated when a full size prototype exists, however.

5.4 Wire Creep

Although the melting point of aluminum is 640°C, the metal loses strength at much lower temperatures resulting in a long term increase in the wire length after repeated heating and cooling under tension ("creep"). Test wires under tension were cycled to high temperature, and the length remeasured after the wire had cooled. The results of some tests are shown in Figure 26.

The unanodized EC-H18 wire was only at high temperature for a week

total, and longer term tests are needed. However, the only significant creep was seen above 220°C, and our current estimate for an operating point is around 190°C. The wire must be spring mounted in any case to take up the length change as the temperature increases from 20°C to 190°C, which is equivalent to a fractional creep of 0.3%.

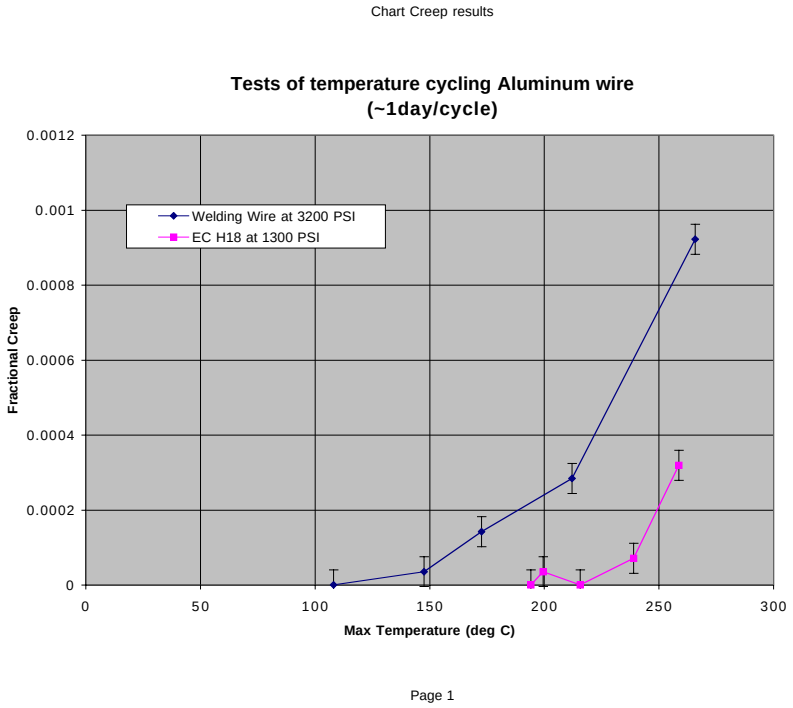

Figure 26: Fractional lengthening (creep) of the Hadronic Hose wire when cycled to high temperature and back to room temperature.

(Note added: some creep has now been observed with the anodized EC-H18 wire, leading to the desire to back off from the above operating conditions somewhat. See Appendix C.)

5.5 Wire Sag and Tension

Since wire sag is a form of misalignment, the misalignment Monte Carlo results would imply that the sag of the wire between supports should be limited to of order 2 mm, which would give an RMS less than 1 mm.

Sag is reduced by increasing wire tension and/or by increasing the number

of wire support spiders. Excess tension leads to creep and wire failure, while extra supports cost installation time and money, and put more material in the beam.

Treating the wire as a limp string with the density of aluminum, the sag δ in mm due to gravity is given by $\delta = 480L^2/\sigma$ where L is the distance between supports in m and σ is the wire tension per unit area in PSI. This gives $\delta =$ 1.8 mm for L = 2.2 m and $\sigma = 1300$ PSI. The tension on a 1.2 mm radius wire is 9 lbs.

With unanodized aluminum EC-H18 wire in the test stand, significant creep was observed at T=130 ^{o}C with a tension of 2600 PSI, but creep was not observed at T=200 ^{o}C with only 1300 PSI. Further testing can refine what an allowable tension would be, but for now we take 1300 PSI as the operating point, which implies that supports are needed approximately every 2 m. (Note added: just before release of this document, some creep was observed with anodized wire, indicating that perhaps the tension should be reduced somewhat).

5.6 Decay Pipe Inductance

The current runs down the wire and returns through the iron decay pipe wall. The voltage needed to produce a short pulse depends partly on the inductance of this coaxial line. The inductance can have an effect both on the design of the power supply and on the allowable length of each wire segment, since the voltage on each segment must be below the breakdown voltage.

The inductance per meter of the wire is:

$$L_{wire} = \frac{\mu_0}{8\pi} = 5 \times 10^{-8}\text{henry/m}$$

where $\mu_0 = 4\pi \times 10^{-7}$ N/A^2.

The inductance per meter of the vacuum space between the inner and outer conductors, which dominates the total inductance, is

$$L_{vac} = \frac{\mu_0}{2\pi} \ln(\frac{r_{pipe}}{r_{wire}}) = 1.34 \times 10^{-6}\text{henry/m}$$

for the radii $r_{wire} = 1.2$ mm and $r_{pipe} = 1$ m.

The inductance of the outer conductor is increased because of the permeability of the iron. For a DC case, the inductance in fact turns out to be large. In our pulsed case however, the current will be confined to a small region on the inner surface of the conductor, and the AC inductance luckily turns out to be small. The permeability of the iron is not well known at this time, so we will calculate inductance over the range $\mu_{rel} = 500$ to 5000. The pulse shape is also

not well defined at this time, but the components would be in the frequency range of from f = 100 Hz (which is the Horn pulse fundamental) to 1000 Hz. The inductance per meter is given by[10]

$$L_{iron} = \frac{1}{4\pi^2 \rho \delta f r_{pipe}} \frac{\sinh(x) - \sin(x)}{\cosh(x) - \cos(x)}$$

where ρ is the electrical conductivity, taken to be 1.2×10^7 mho/m, $\delta = 1/\sqrt{\rho \pi f \mu_{rel} \mu_0}$ is the skin depth, and $x = 2d/\delta$ is a scaling variable and d is the thickness of the pipe. (The trigonometric factor is 1 in our parameter region, the precise value of d does not affect the result since d is so much larger than the skin depth). The resistance per meter of the iron is given by:

$$R_{pipe} = \frac{1}{2\pi r_{pipe} \delta \rho} \frac{\sinh(x) + \sin(x)}{\cosh(x) - \cos(x)}.$$

As seen in Table 3 the inductance of the iron is at least an order of magnitude less than L_{vac}, and can thus be ignored.

μ_{rel} of iron	f (Hz)	δ (m)	R_{pipe} (Ω/m)	L_{iron} (henry/m)
500	100	6.6×10^{-4}	2.1×10^{-5}	3.3×10^{-8}
500	1000	2.1×10^{-4}	6.6×10^{-5}	1.0×10^{-8}
5000	100	2.1×10^{-4}	6.6×10^{-5}	1.0×10^{-7}
5000	1000	6.6×10^{-5}	2.1×10^{-4}	3.3×10^{-8}

Table 3: Contribution of the iron decay pipe to the inductance, as a function of iron permeability and pulse frequency.

For 1000 Amp current, the resistive voltage drop from the iron decay pipe appears to be at most a couple of volts per section, or in the most extreme case about 140 volts from one end of the decay pipe to the other.

Note that none of these numbers have been corrected for the change in resistivity of iron when it is heated by the beam, but that will be a small effect since the total inductance is dominated by L_{vac} and the total resistance is dominated by the wire resistance.

5.7 Wire Supports

The current design of the hose includes the following items:

- Small support brackets would be welded or nailed to the iron decay pipe. Each support bracket would have an alignment tooling ball socket and an adjustable eyebolt for tensioning/aligning a support wire. The support wire is attached through the eye inside a ceramic insulator that provides electrical isolation.

- The tripod of support wires from one end of the Hose wire is anchored solidly to wall brackets. At the other end, constant tension springs at the eyebolts connect to the tripod, so that expansion of the wire can be taken up.

- Every 2.2 m, a support spider holds the Hose wire centered. The three-way support consists of three wire loops, which interlock around the Hose wire. This eliminates the need for any widget at the Hose wire, and minimizes mass at small radius,

Note the brackets, springs and insulators are kept at large radius in the decay pipe, so that their effect on the beam is negligible.

5.8 Power Supply

Detailed engineering of the power supply has not been done, but a reference design based on an existing power supply has been developed.

In this design 700 V from the power supplies at the end of the decay tunnel feed transformers located along the decay pipe, which then serve to both convert the power to low voltage high current and provide isolation to each wire segment. The higher supply voltage is used in order to reduce the cost of the long cable runs down the decay tunnel.

Five units of the type of power supply used for the flashlamp for the photoinjector project[11] would provide 160 Volts at 1000 Amps to each of 60 wire segments, and are used in the cost estimate. The transformer cost is currently based on two segments sharing the same transformer core.

Each power supply unit takes up around 2'x3' of floor space and is 3' high, so that a space of 10'x3' plus aisle would be required.

Of order 6 kw of power is being drawn from the supplies.

5.9 Further R&D

The following is a list of hardware related tasks that should be done before construction begins:

- Do more creep versus temperature tests on the wire, including alternative types of wire (see Appendix B).
- Build and operate a full scale prototype of a wire segment in a 2 m diameter pipe.
- Work out a detailed installation and alignment proceedure, including proceedures to keep the wire straight during installation.
- Obtain a more complete understanding of the environmental conditions, i.e. a more detailed model to derive decay pipe operating temperature, and a study of possible motion of the decay pipe.

6 Survey and Alignment

The Hadronic Hose alignment goal is ± 2.0 mm maximum deviation of the central conductor from a straight line, which is set to minimize the intersection of particle orbits with the wire. (The alignment tolerance of this line to the direction of Soudan is considerably more relaxed). Every 2.2 m along the decay pipe, 3 brackets, spaced 120 degrees at 12, 4, 8 o'clock, will be welded to the inside of the pipe. Each bracket will have an attachment point for a radial support wire for the central conductor and a 1/4 inch diameter hole to insert a tooling ball for alignment. Before the decay pipe is installed, an alignment network will be setup in the tunnel. This will be needed both to correctly position the decay pipe and to increase the accuracy of the internal alignment network. After the decay pipe is in place and encased in concrete and before the central conductor is installed, a survey crew will start at one end and proceed internally down the pipe to the other end, measuring the location of a tooling ball in every bracket. It is estimated that 15 alignment crew shifts will be required to complete this. Pre-analysis shows that this would yield the tooling ball positions accurate to ± 4.0 mm (2 sigma) halfway along the decay pipe. If this internal network is tied through a power feed through port to the external network in the decay tunnel halfway down, this accuracy becomes ± 1.3 mm. To achieve more alignment tolerance safety factor, the internal network will be be tied to the external decay tunnel network at 3 places (1/4, 1/2, 3/4 points along the decay pipe) which would give an accuracy of 0.5 mm. As each 11 m central conductor section is installed, it will be positioned by making stickmike measurements, accurate to 0.2 mm, to tooling balls in each of the three brackets at each position along the section.

7 Radiation Protection

A Monte Carlo calculation using the MARS code has been done to demonstrate the adequacy of the current decay pipe shielding design given the Hadronic Hose. The shielding is to protect the groundwater from irradiation. The star density in the rock outside the decay pipe is calculated to be modestly (factor of 1.1 to 1.5) larger with the Hadronic Hose. This is a small enough increase that no extra shielding is felt to be required, although it puts the design at the limit of the agreed upon safety factor.

A second aspect of Radiation Protection is that after any significant amount of running, the interior of the decay pipe will be too radioactive to access for any human repair of the Hadronic Hose. Monte Carlo simulations of running the Hadronic Hose with segments turned off have been made with results shown in Sec. 4.5. Consideration of possible remote robotic repair is also being made [12].

8 Monitoring

Several forms of monitoring are envisioned:

- The power supplies will have voltage and current monitoring, and be set to trip if either is out of range.
- A small number of thermocouples will be used to monitor the temperature of the decay pipe.
- The decay pipe would have vacuum monitoring in any case; for Hadronic Hose some form of feed-back to keep the vacuum constant would be desirable if aluminum wire is used.
- The Hose will give characteristic signatures in the muon monitor chambers and the hadron monitor chamber at the end of the decay pipe.

Other forms of monitoring are possible:

- A few extra feed-through ports, with windows instead of feed-throughs, may be used to occasionally check the alignment of a sample of points on the wire.
- Relative alignment could also be monitored continuously in some places by use of pickup coils.
- If robotic repair is possible, then remote robotic check of alignment would be possible during extended shutdown periods.

9 Cost Estimate

The following are rough estimates of the cost of various components of the Hadronic Hose. Electrical monitoring is included in the cost of the power supply. No overhead or engineering is included, and the list is probably not comprehensive, but it indicates the scale of the project is of order $1 million.

Wire	$ 8 k
Misc. hardware	$ 60 k
Tech. installation	$ 60 k
Power supply	$ 87 k
Transformers	$ 75 k
Power cable	$ 60 k
Power cable tray	$ 100 k
Survey crew	$ 20 k
Vacuum electrical feedthrough	$ 6 k
Feedthrough mechanical	$ 20 k
Electrical engineering	?
Mechanical engineering	?
Space for power supply	?

Table 4: Partial cost estimate.

10 Installation and Schedule Implications

The 60 feed-throughs which penetrate the 2 m concrete shielding into the decay pipe have to be added to the civil construction package. An estimate has not yet been made of the time this adds to the construction. The amount of welding involved is fairly small compared to the welding together of the decay pipe sections, and could possibly be done in parallel with that welding, and should thus be a fairly minor schedule impact.

The alignment survey inside the decay pipe and the installation of the wire is roughly estimated to take 45 shifts. This can be done mostly in parallel with the installation of the target pile and the installation of the near detector, and thus should have only minor schedule implications.

The Hadronic Hose installation does not require very much use of the access shaft and crane, which is why major schedule conflicts are not forseen.

One item which needs to be better understood is the relation between vacuum testing, with the need for installation of the decay pipe end walls, and installation of the Hadronic Hose. A scenerio for the order of activities which appears to fold in reasonably with other installation efforts is (i) survey/alignment inside pipe, (ii) installation of end caps, (iii) vacuum testing, (iv) hose installation. This would require either access ports separate from the end caps, or end caps that can be removed. This does not however sound like a show-stopper.

11 Conclusion

To conclude we summarize the potential benefits of adding the Hadronic Hose to the NuMI baseline beam line:

- **Reduction of Hadron Production Uncertainty** This is the primary motivation for Hadronic Hose. Please refer to the proceeding sections for the details.

- **Reduction of Mechanical and Electrical Tolerances** Several mechanical tolerances are eased by the Hadronic Hose. For instance, the effect of an induced field in the central hole of the horn due to thickness variations in the inner conductor (which is perhaps the hardest tolerance to meet that we know of) is reduced by a factor of two compared to the baseline configuration.

- **Improved Event Rate for Low Energy Beam** The ν_μ CC spectrum is plotted with and with out the addition of the Hadronic Hose in Figure 1 for the PH2ME beam, and in Figure 27 for the PH2LE beam. For the Medium Energy beam configuration, the Hadronic Hose gives an 18% increase in the event rate compared to the baseline beam, and for the Low Energy beam configuration, the increase in event rate is roughly 28% for $E_\nu < 6$ GeV. This is a significant increase especially for the Low Energy beam configuration, which is most sensitive in the low Δm^2 region and is statistics limited. While the Hadronic Hose cost is not known very well, it appears small compared to the cost of more detector mass to get a similar increase in rate.

- **Reduction of Other Systemmatic Uncertainies in Neutrino Oscillation Measurements** Several possible systematic uncertainties involve second order effects, which are a combination of beam far-near differences and some other aspect of the experiment. An example is the uncertainty in neutrino interaction cross sections. If the near and far spectrum shapes

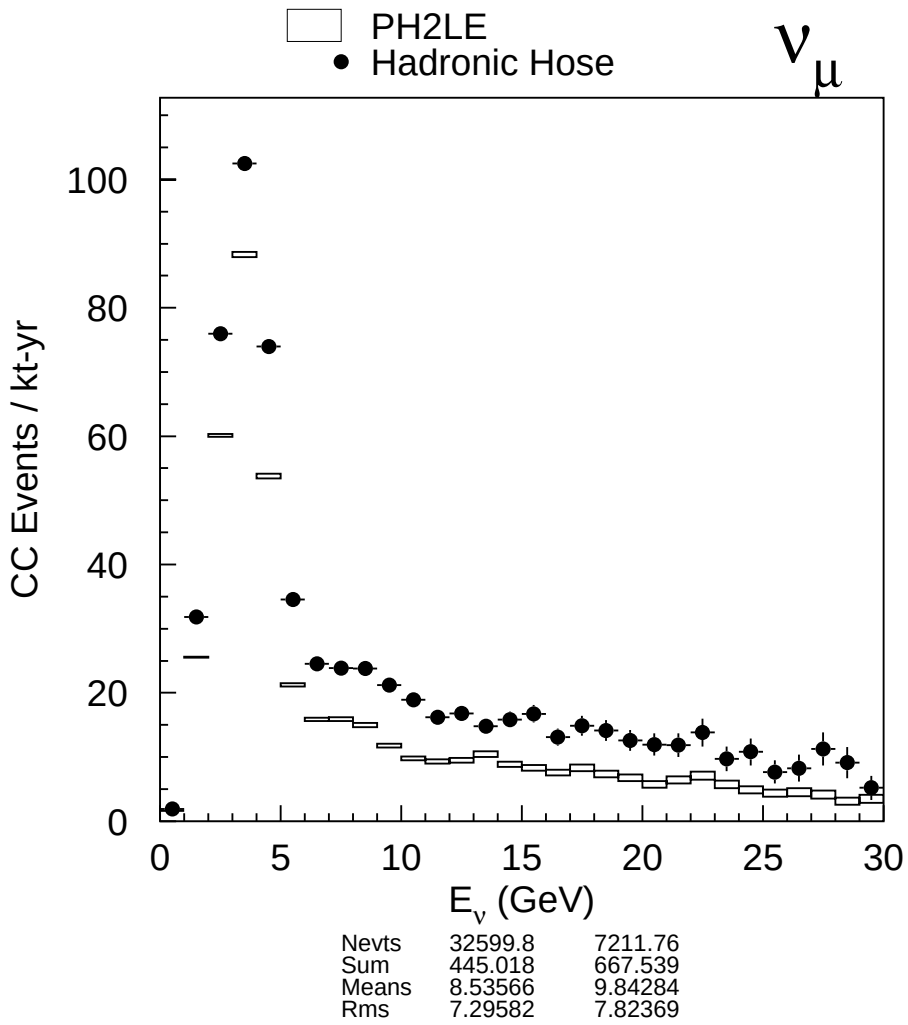

Figure 27: The low energy beam far detector ν_μ CC spectrum. The baseline low energy beam is shown by boxes and the baseline with the addition of the Hadronic Hose is shown by the points.

are identical, then uncertainty in the energy dependence of the cross sections should cancel out in the far-near comparisons. If the near and far spectrum shapes are different, then a systematic uncertainty can appear. Other examples of uncertainties which would cancel if the near and far spectrum were identical are uncertanties in the reconstruction efficiencies and detector resolution.

- **Perception of the Scientific Community** The idea of having simple comparisons between near and far detectors is central to the MINOS experiment. With a Hadronic Hose, one can compare the spectra in the near and far detectors to see oscillation signals without making Monte Carlo corrections for beam effects. A simple hand calculation of the integral of the pion lifetime over the length of the decay pipe is sufficient correction for all except the most detailed and precise studies. Presentation of the results should also be easier.

The benefits of the Hadronic Hose are to be weighed against the potential draw backs; everything has its price, and Hadronic Hose is no exception. First, there is the dollar cost, of which no good estimate has yet been made. Second, there could easily be a two-month schedule implication due to installation time. A possible physics objection is that that the ν_e background is increased by a factor of 1.5. Potential risks include failure of the Hadronic Hose after a significant amount of data has been collected. This would force the collaboration to analyze two sets of data with different systematics. Also, it is one more system to commission, and to have to maintain. One feature of the Hadronic Hose is that if it does not work, it can simply be turned off – an installed Hose does not interfere with the standard operation of the baseline beam. This limits the risk of failure.

The addition of the Hadronic Hose to the NuMI baseline has the potential to improve the far-near spectrum comparison, reducing the systematic uncertainties relevant to neutrino oscillation measurements. In particular, the Hadronic Hose reduces the sensitivity of the far-near comparison to the hadronic production p_t spectrum. The additional focusing provided by the Hadronic Hose also has the potential to increase the neutrino event rates by 18% for the medium energy beam configuration and 28% in the low energy beam configuration. Simulations of the performance of the Hadronic Hose suggest that alignment tolerances are within reach. Potential drawbacks to the Hadronic Hose are cost, schedule and risk, as well as an increase in the electron neutrino contamination. We believe these drawbacks are out-weighed by the gains.

References

[1] R. H. Milburn, "Theory of the Hylen Hadronic Hose", NuMI-B-271, May 28, 1997.

[2] A.E. Brenner *et al.*, Phys. Rev. D26 (1982) 1497.

[3] C.L. Wang, Phys. Rev. **D10**, 3876 (1974).

[4] G. Cocconi *et al.*, LBL Report No. UCRL 10022, (1961).

[5] A.J. Malensek, "Empirical Formula for Thick Target Particle Production", Fermilab FN-341, October 12, 1981.

[6] G. Collazuol *et al.*, "Neutrino Beams: Production Models and Experimental Data", CERN-OPEN-98-032.

[7] The NA56/SPY Collaboration, CERN-EP/99-19, February 1, 1999.

[8] H.W. Atherton *et al.*, CERN 80:07, (1980).

[9] A. Van Ginnekin, "CASIM - Program to Simulate Transport of Hadronic Cascades in Bulk Matter", Internal Fermilab Report FN-272, 1975.

[10] K.Simonyi, "Theoretishe elektrotechnick" 1956, Veb Deutsher Verlag der Wissenschaften, Berlin.

[11] H. Pfeffer, private communication, April 18, 1997.

[12] S. Childress, J. Anderson Jr., C. Kendziora, "Robotic Repair for NuMI Hadronic Hose", NuMI-B-546, October 1999.

A Appendix: Single Turn Extraction

There is a reasonable possibility that the baseline beam extraction for NUMI will be changed from 1 ms resonant extraction to 8 μs single turn extraction. In this case, the current pulse to the Hadronic Hose wire could be shortened, reducing the heating by a factor of around 4. This extra headroom could be used either as an extra safety factor (Figure 24), or to allow the increase of wire instantaneous current by a factor of 2 to 2 kA to get a higher event rate for Low Energy beam (Figure 10).

B Appendix: Alternate Wire Materials

With some reduction in tension or current, the anodized EC-H18 aluminum is a viable condidate for the Hadronic Hose operation. However, a wire with a greater safety factor would be desirable. There are several candidates which should be examined before the final wire type is selected. Examples include:

- Series 8000 aluminum is supposed to have the same conductivity and density as EC, but be less susceptable to creep at high temperatures, and is thus an attractive possibility.
- An alloy of Beryllium with 38% aluminum has somewhat less conductivity, but would have less beam heating and should work better at higher temperatures. This is also an attractive possibility.
- Tungsten can withstand very high temperatures and remain strong. Several properties make it problematic, but tungsten is still a possibility.

C Appendix: Prototype Operation Scaled to Beam Conditions

To assure that there is a set of hardware parameters for which Hadronic Hose works, the anodized prototype wire was operated at temperature, stress, and vacuum conditions as close as possible to that expected for real operation. It is impossible to make all conditions identical however, so a careful explanation of the extrapolation involved is given here.

Since the test stand is not in a beam line, the effect of beam heating is calculated using a Monte Carlo and is accounted for as follows: an excess current is sent through the wire to give equivalent heating of the wire, and heating tape is wrapped around the test stand pipe to raise it to the calculated decay pipe temperature.

Beyond the calculation of the beam heating, three assumptions are made:

- The resistance of the wire is inversely proportional to the cross sectional area of the wire. (The skin depth of aluminum is much larger than the wire radius for the frequencies involved, so this is a good assumption).
- The rate of heat loss of the wire is proportional to the surface area of the wire.
- The beam heating is proportional to the cross sectional area of the wire. (The beam heating Monte Carlo was only run with a 1 mm radius wire).

The 1000 Amp 1.3 ms pulse every 1.9 seconds is the equivalent of 26 Amps D.C. We have 0.8 mm radius wire in the test stand instead of the 1.2 mm radius wire which is expected to be used in the operational Hose, so to have the equivalent heat flow per unit area requires 14 Amps D.C. This would assure that the heat flow and equalibrium temperature were the same as in the actual Hose, excluding beam heating. Up to this point, no extra assumptions are required about conductivity of the wire at a given temperature, or the way cooling by radiation or gas scale with temperature, and the actual temperature of the wire does not need to be known.

The temperature drop across the concrete shielding to conduct out the power hitting the decay pipe walls is calculated to be 17°C. Making the further assumption that the decay pipe tunnel is 90°F (32° C), the decay pipe wall should be 49°C. In the test, the pipe wall was maintained at 51° C using heating tape.

According to the CASIM Monte Carlo, beam heating of the wire in the upstream region of the Hadronic Hose (excluding the first meters) is 2.3 J/cm^3 for 4×10^{13} protons on target . The design repetition rate is 1.9 seconds. Thus the heat given off from the surface of a 0.12 mm radius wire must be 0.073 w/cm^2. Using a resistivity of 4.3×10^{-6}, corresponding to aluminum at a temperature of 180 °C, it takes 13 Amps D.C. in the 0.8 mm radius test wire to produce the same power per unit surface area. Combining this with the 14 Amp Hose current above leads to a total of 19 Amps required to simulate actual hose conditions.

The anodized hose wire was run at the above conditions for 9 days. At the end of that time, the wire was measured to have stretched 0.025±0.010 inches out of 141 inches, or a fractional creep of 1.8×10^{-4}. Assuming the creep is real (e.g. did not happen at the crimp joint) and assuming a linear relationship over time for the creep, operation of 270 days/year for four years would result in creep of 2%. Although the spring system can be designed to take up this much creep, we feel it is necessary to reduce the creep by some combination of (i) reduction of the wire tension, (ii) reduction of the wire temperature - either less current (perhaps only in the first segment) or switch to short spill extraction, and (iii) switch to a wire alloy less susceptable to creep.

This result was obtained at too late a time to revise the rest of the document before the October collaboration meeting.

It is clear that much more extensive testing of wires under different conditions is needed over the next year, but heating a set of wires e.g. in an oven under different tension and temperature conditions does not appear a very costly or technically risky venture.